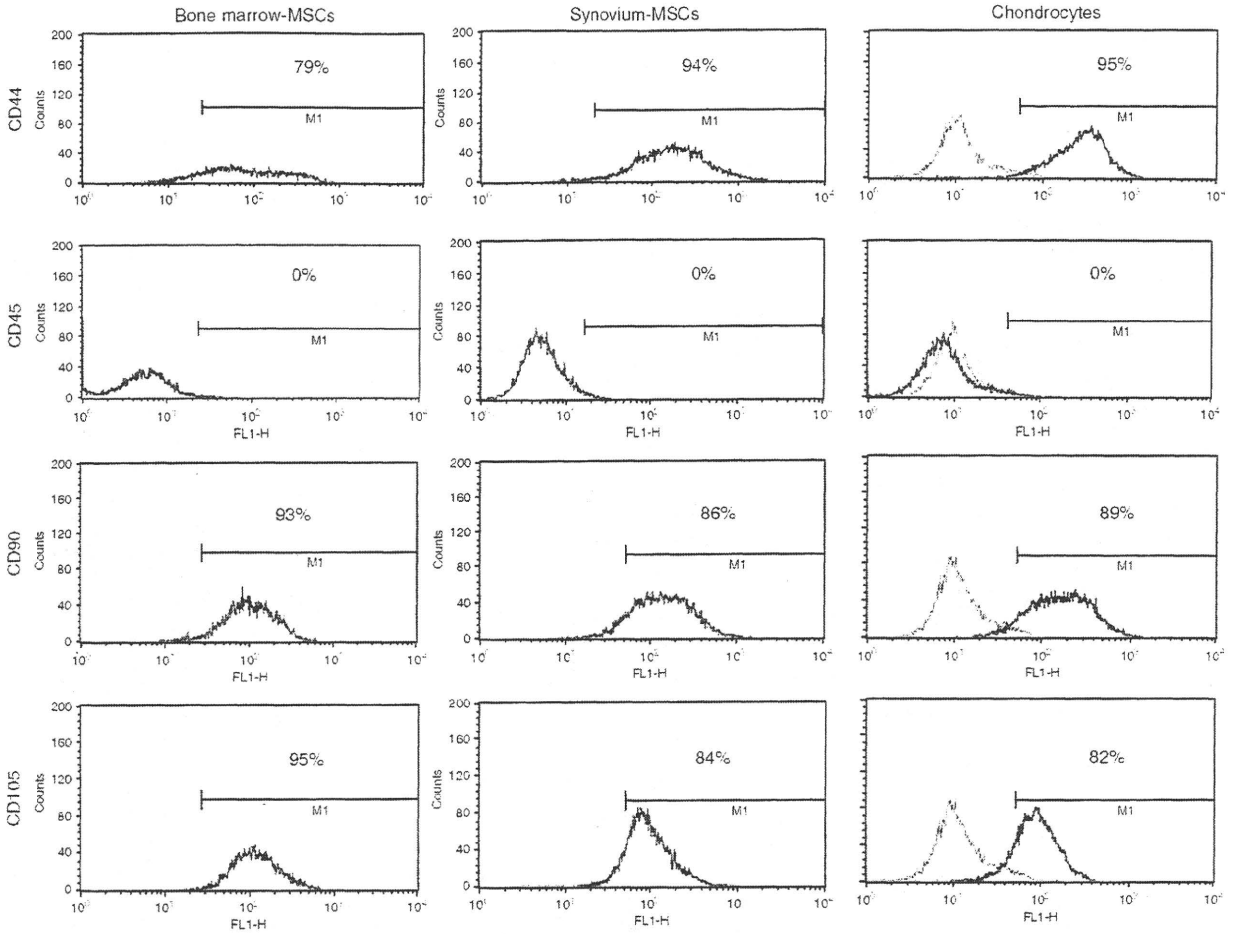

Figure 2 Surface epitopes of bone marrow-, synovium-MSCs, and chondrocytes. Representative histograms are shown as an open plot, and isotype controls are shown as gray.

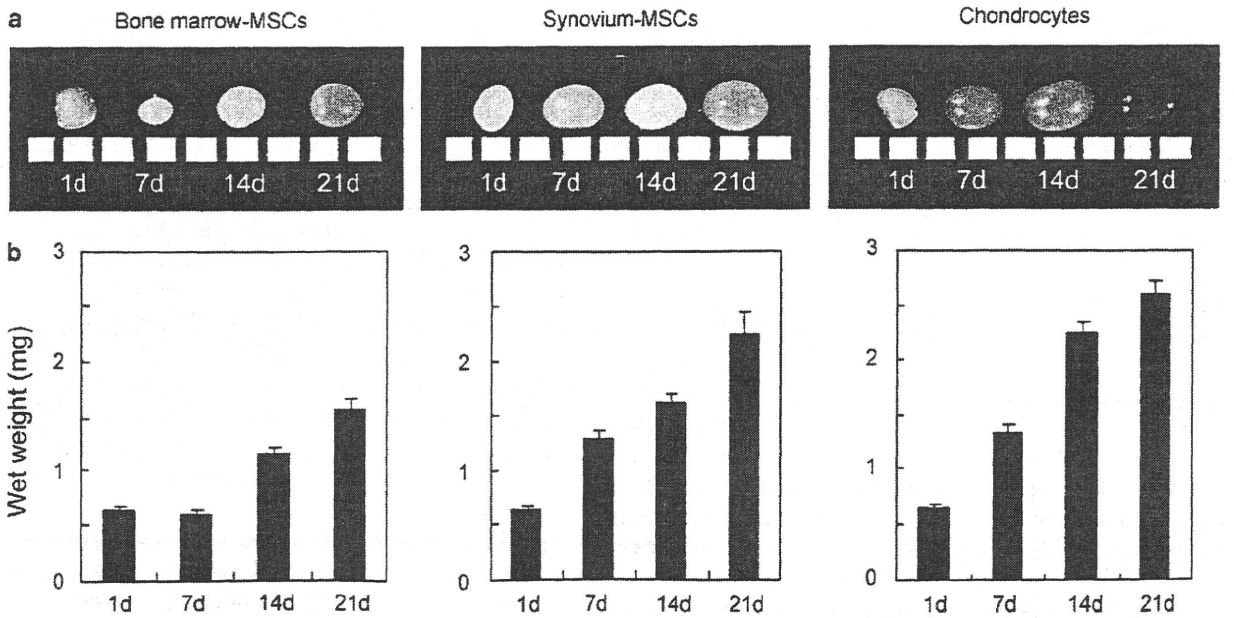

Figure 3 Time course of *in vitro* chondrogenesis of bone marrow-, synovium-MSCs, and chondrocytes. (**a**) Macro pictures of pellets with a 1-mm scale. (**b**) Wet weight of pellets. The data are expressed as mean ± s.d. ($n = 3$).

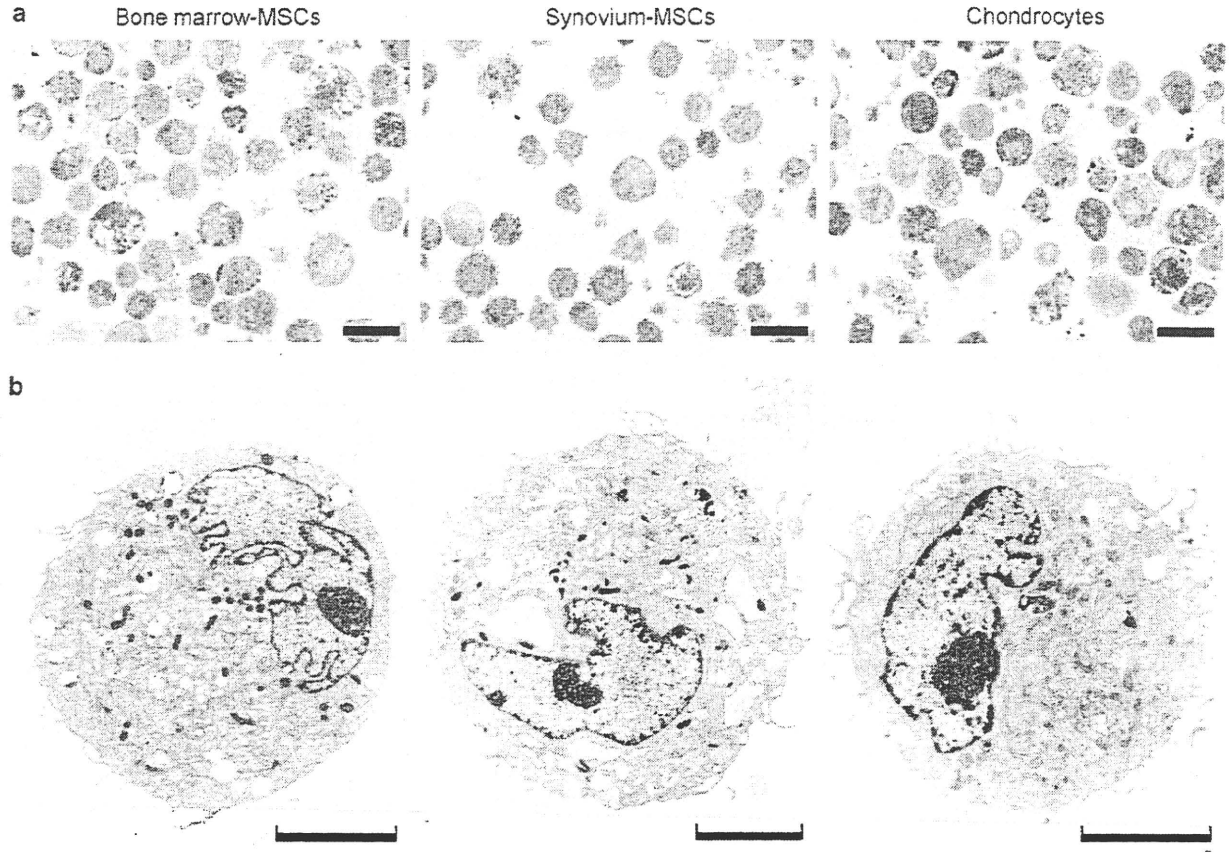

Figure 4 Morphology of bone marrow-, synovium-MSCs, and chondrocytes before induction of chondrogenesis. (**a**) Optical micrographs of the cells stained with toluidine blue. Scale bar = 20 μm. (**b**) TEM images. Scale bar = 5 μm.

observed by transmission electron microscopy images in the deep zone in the three populations. The cells with irregular contours were surrounded by well-developed matrix fibers (Figure 7c). Neither TUNEL positive nor Ki67 positive cells were observed. Immunoelectron microscopy at day 21 demonstrated only slight expression of type I collagen, and higher expression of type II, X collagen, and chondroitin sulfate in the deep zone in the three populations (Figure 8).

DISCUSSION

In this study, we compared the morphology of bone marrow-MSCs, synovium-MSCs, and chondrocytes during their *in vitro* chondrogenesis (Table 1; Figure 9). Before induction for chondrogenesis, trypsinized cells looked similar among the three populations.

At day 1 (aggregation phase), the structure of the three masses was divided into two layers, and the most obvious differences in the three populations were observed at the deep zone. In bone marrow-MSCs, round cells accumulated without intercellular space, and the cells were mainly connected through intermediate junctions. In synovium-MSCs, elongated cells accumulated with small desmosomes, and intercellular spaces could occasionally be seen. In chondrocytes, separated oval and polygonal cells were connected only in a narrow spotty area through a small desmosome.

At day 7 (early phase of differentiation), the structure of the three masses was divided into three layers, and the most obvious differences in the three populations were observed at the middle zone. In bone marrow-MSCs, the middle zone consisted of dense smaller cells and apoptotic cells. In synovium-MSCs, the middle zone consisted of dense arrayed wider cells and apoptotic cells. In chondrocytes, the middle zone was acellular without apoptotic cells.

At day 21 (late phase of differentiation), the morphology of cells and extracellular space became similar in that each cell was located separately with abundant extracellular matrix. The superficial zone was still obvious in bone marrow-MSCs, but hardly seen both in synovium-MSCs and chondrocytes.

At the early phase, apoptotic cells were observed in the middle zone. The gradient of oxygen, cytokines, or other nutrients presumably affects the fate of the cells,[19] and the middle zone might be an inappropriate environment for the cells located there. If this is the case, why were there no apoptotic cells of chondrocytes in the middle zone? One

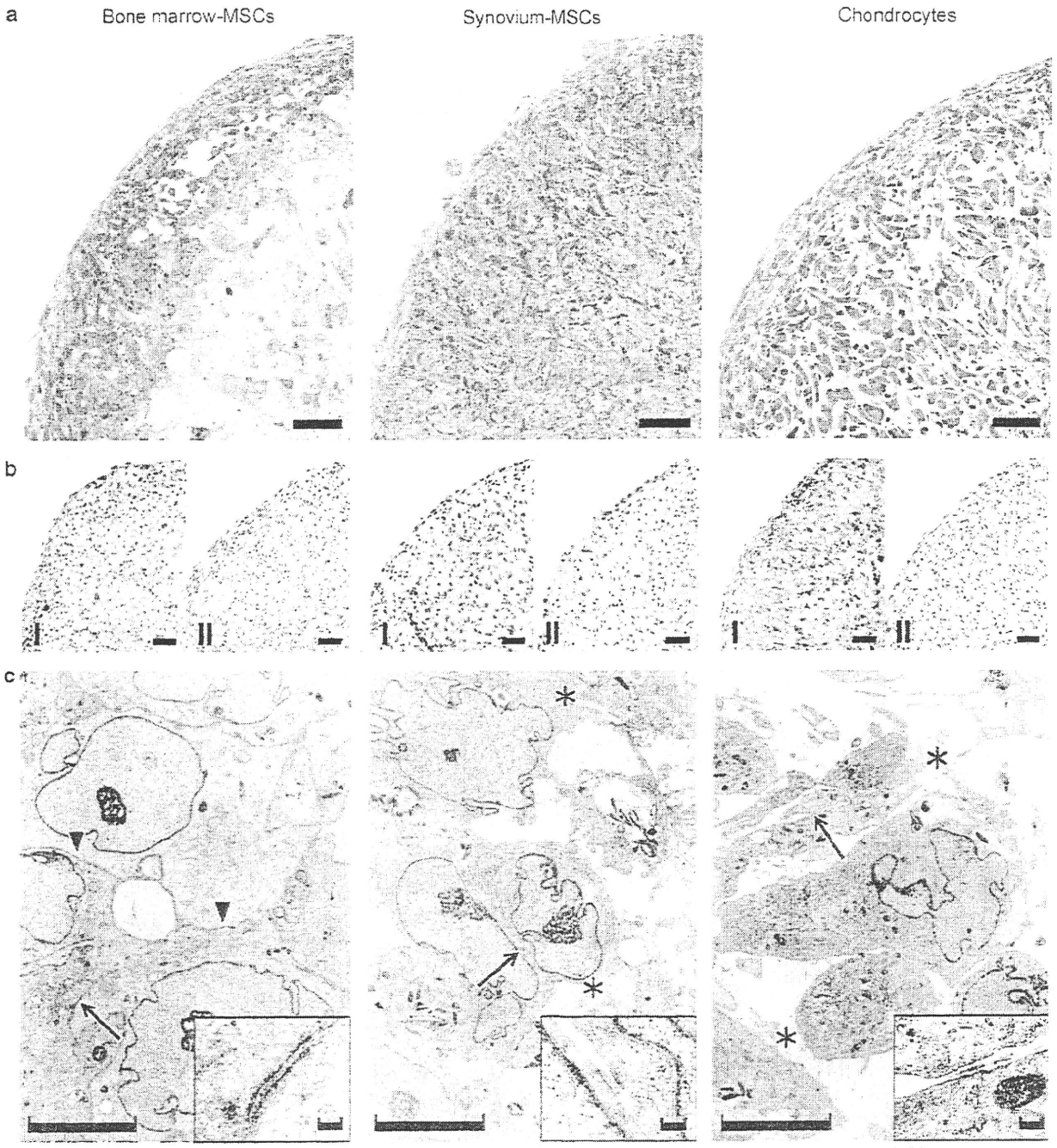

Figure 5 Morphology of pellets 1 day after induction of *in vitro* chondrogenesis. **(a)** Optical micrographs of pellets stained with toluidine blue. Scale bar = 50 μm. **(b)** Immunohistochemical staining for type I and II collagen. Scale bar = 50 μm. **(c)** TEM images of pellets in the deep zone. Scale bar = 5 μm. In bone marrow-MSCs, intermediate junctions are shown as arrow heads, and desmosome as arrow. In synovium-MSCs and chondrocytes, small desmosomes are shown as arrow and type I collagen fibers as asterisks. Desmosome and small desmosomes are magnified. Scale bar = 100 nm.

possibility is that chondrocytes do not die due to apoptosis during *in vitro* chondrogenesis. Tallheden *et al*[22] reported that chondrocytes did not express apoptosis-related genes during *in vitro* chondrognesis.

In bone marrow- and synovium-MSCs, we observed TUNEL positive cells at day 7 and no TUNEL positive cells at day 21. In our earlier reports, DNA content decreased largely within the first week and only slightly between 2 and 3 weeks during *in vitro* chondrogenesis of MSCs derived from bone marrow[17] and synovium.[23] The results of TUNEL assay in this study and the results of DNA content assays in earlier reports indicate one possibility that viable cells decreased

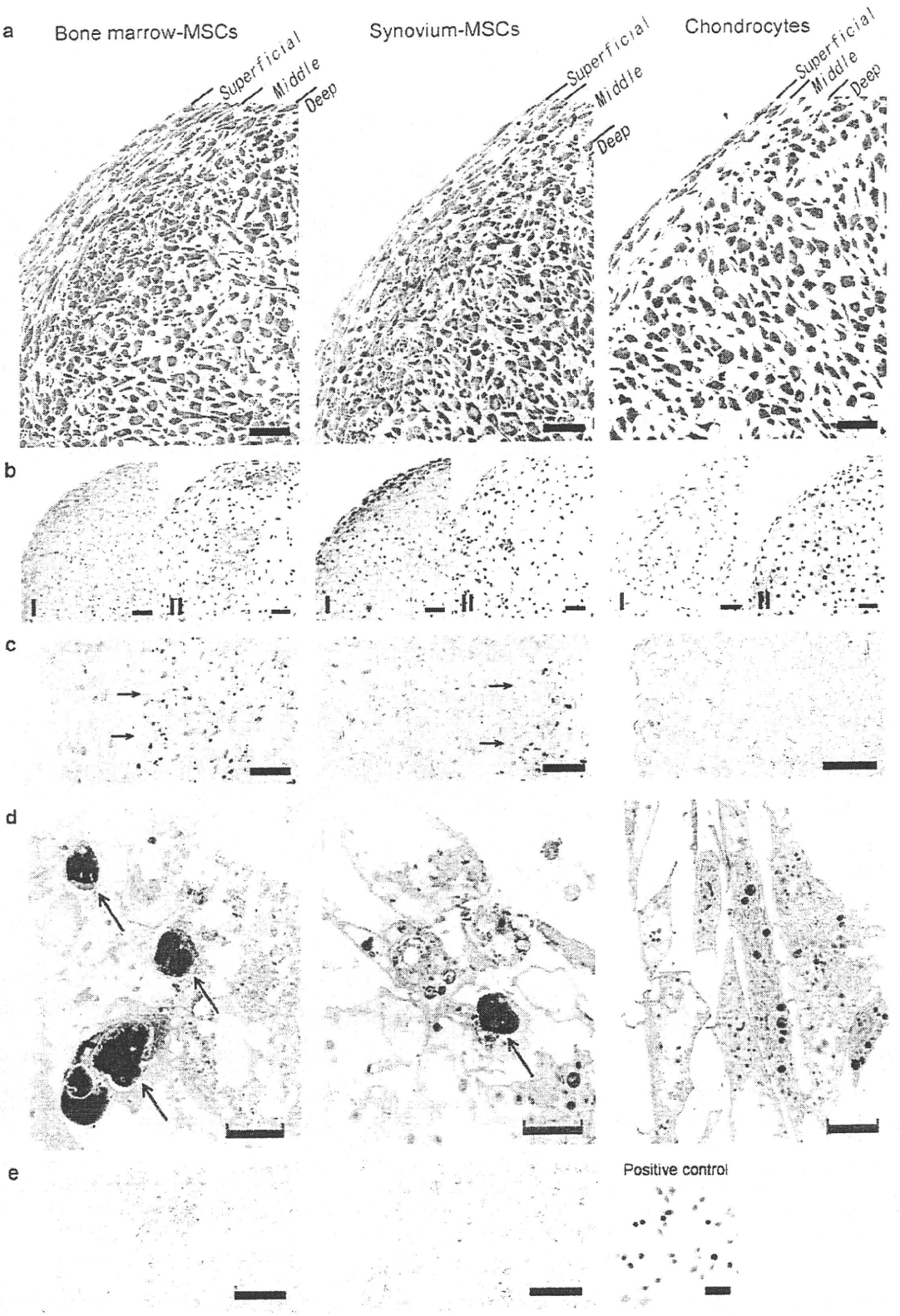

Figure 6 Morphology of pellets 7 days after induction of *in vitro* chondrogenesis. (**a**) Optical micrographs of pellets stained with toluidine blue. Scale bar = 50 μm. (**b**) Immunohistochemical staining for type I and II collagen. Scale bar = 50 μm. (**c**) TUNEL staining for apoptosis in the superficial and middle zone. TUNEL positive cells are shown as arrows. Scale bar = 50 μm. (**d**) TEM images in the middle zone. Apoptotic cells are shown as arrow. Scale bar = 5 μm. (**e**) Ki67 staining for proliferation in the superficial and middle zone. Hela cells are also shown as positive control. Scale bar = 50 μm.

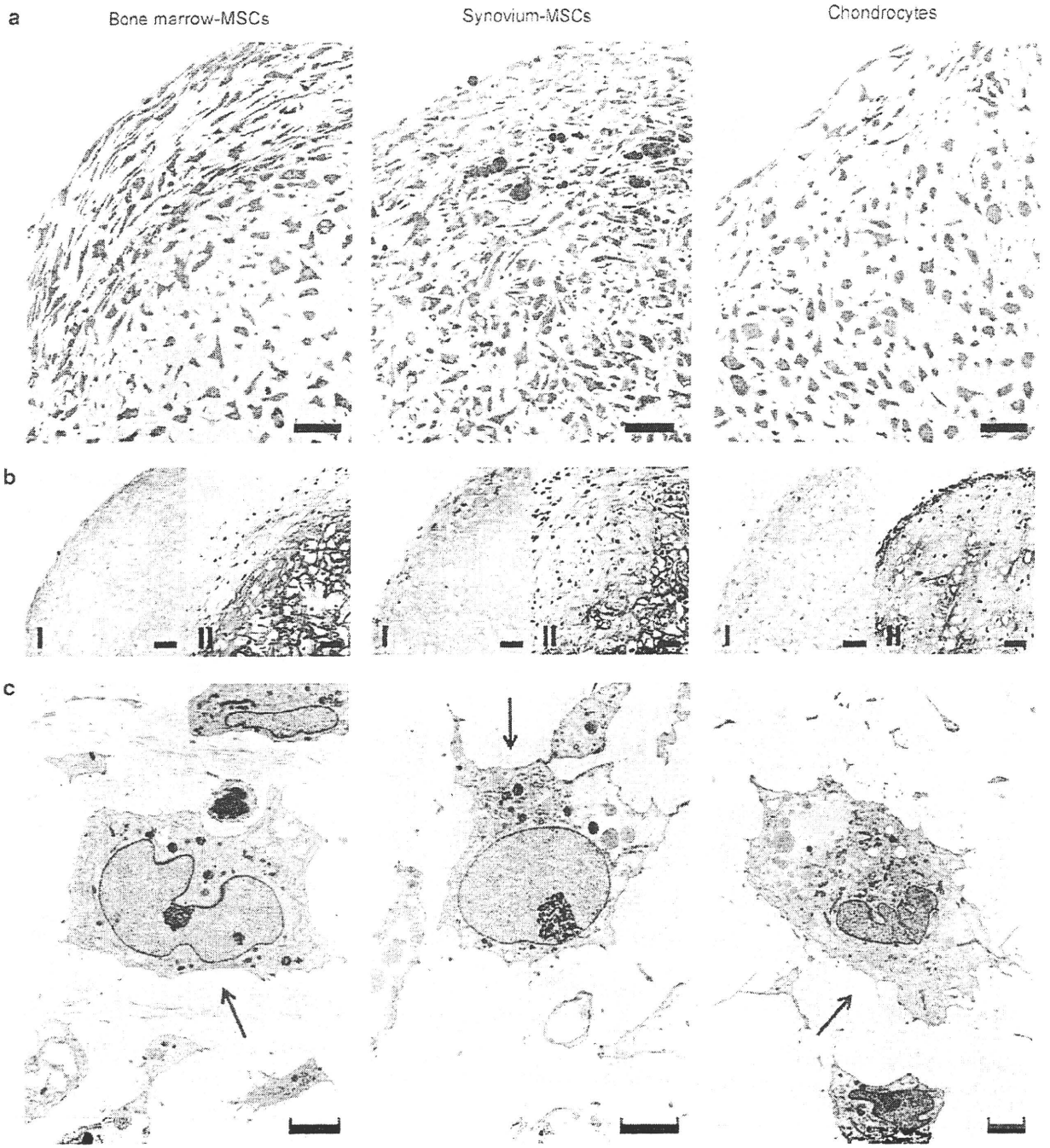

Figure 7 Morphology of pellets 21 days after induction of *in vitro* chondrogenesis. (**a**) Optical micrographs of pellets stained with toluidine blue. Scale bar = 50 μm. (**b**) Immunohistochemical staining for type I and II collagen. Scale bar = 50 μm. (**c**) TEM images in the deep zone. Mature chondrocyte-like cells are located at the center. Well-developed matrix fibers are shown as arrow. Scale bar = 5 μm.

largely within the first week and only slightly between 2 and 3 weeks because of apoptosis.

At the early phase of differentiation, pellets of bone marrow- and synovium-MSCs showed higher density of cells in the middle zone and demonstrated different features from that of chondrocytes. Was there any difference in cell proliferation between the cells? The answer is no. We examined Ki67 expressions for proliferation but did not observe any Ki67 expressions in the three populations. This indicates that different features between two populations of MSCs and chondrocytes in the middle zone were not due to cell proliferation. In our earlier report of bone

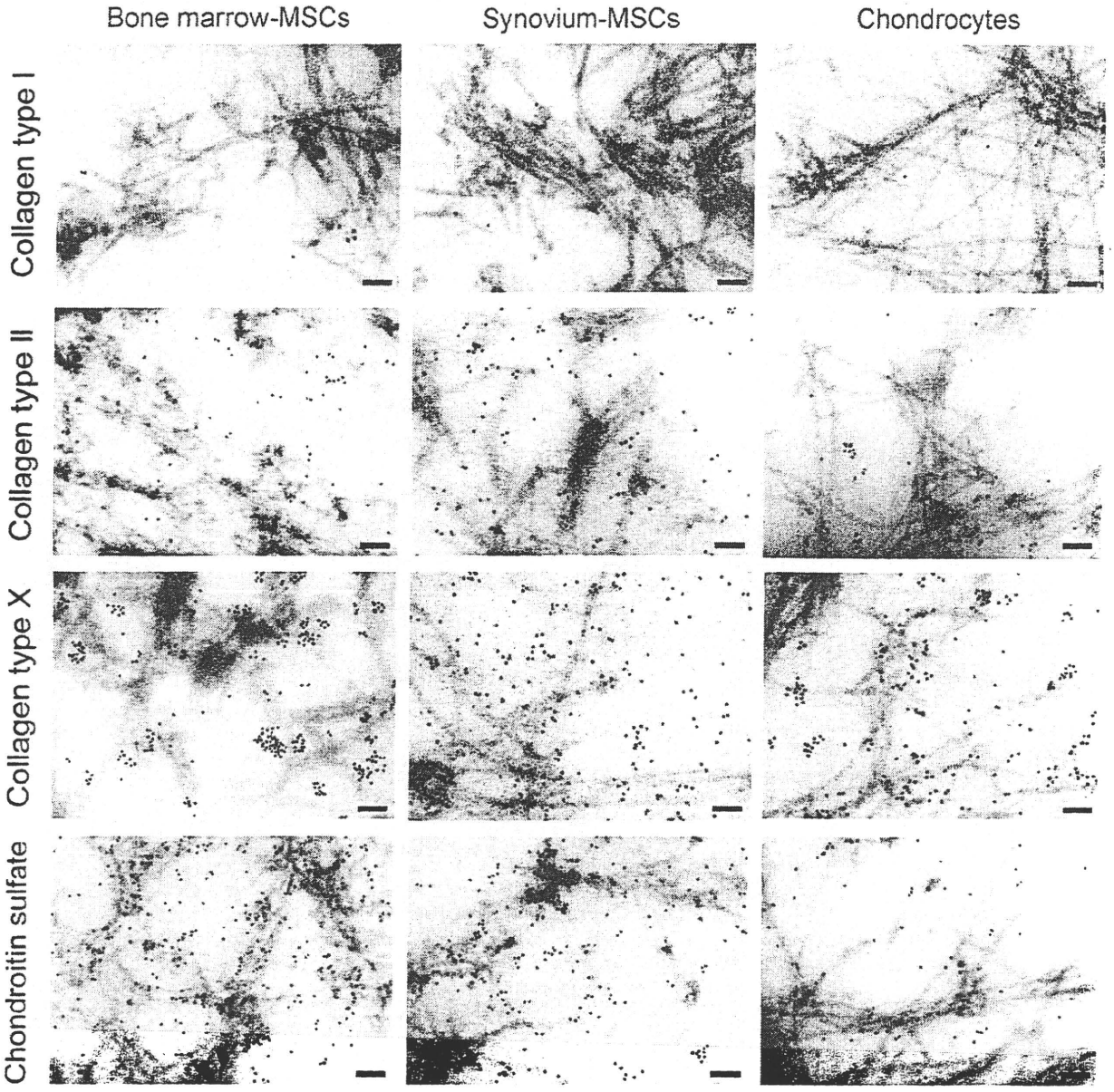

Figure 8 Immunoelectron microscopic images for pellets 21 days after induction of *in vitro* chondrogenesis. Expressions of collagen type I, II, X, and chondroitin sulfate proteoglycan in the deep zone by the gold particle deposition are shown. Scale bar = 100 nm.

marrow-MSCs, a pulse-labeled and chase experiment with [^{3}H] thymidine indicated that there was a 25% decrease in the specific activity of cellular DNA between day 0 and day 7, but thereafter the values remained constant,[17] demonstrating that bone marrow-MSCs did not divide at the early phase.

We performed all experiments in three donors with osteoarthritis, and similar results were obtained. To account for variances among donors and among procedures,[5] we harvested bone marrow, synovium, and cartilage simultaneously after total knee arthroplasty, performed the procedures, and analyzed the cells from bone marrow, synovium, and cartilage at the same time. It would be intriguing to examine whether similar results could be obtained in cells derived from young donors; however, it is not easy to harvest bone marrow, synovium, and especially cartilage from young donors simultaneously. The confirmation in young donors would be practically difficult.

Ectopic cartilage formation is one of the pathological conditions in articular joints.[14] Candidate cell sources for the ectopic cartilage formations are stem cells in bone marrow and synovium, in addition to chondrocytes. A comparison of the morphology of cartilage formation between *in vitro* chondrogenesis of these cells and the ectopic cartilage for-

Table 1 Critical differences of morphologies during *in vitro* chondrogenesis

Days	Zone	Bone marrow-MSCs	Synovium-MSCs	Chondrocytes
0		Round cells with a large number of processes at the cell surface		
1	Superficial zone		Spindle cells parallel to the surface	
	Deep zone	Round cells without intercellular space	Elongated cells with intermediate intercellular spaces	Oval and polygonal cells with intercellular spaces
		Intermediate junctions	Small desmosome	Small desmosome
7	Superficial zone		Spindle cells parallel to the surface	
	Middle zone	Higher cell density	Higher cell density	Lower cell density
		Apoptotic cells	Apoptotic cells	No apoptotic cells
	Deep zone	Intermediate intercellular space	Relatively narrow intercellular space	Large intercellular space
21	Superficial zone	Obvious	Unclear	Narrow
	Deep zone		Polygonal cells with pericellular matrix	

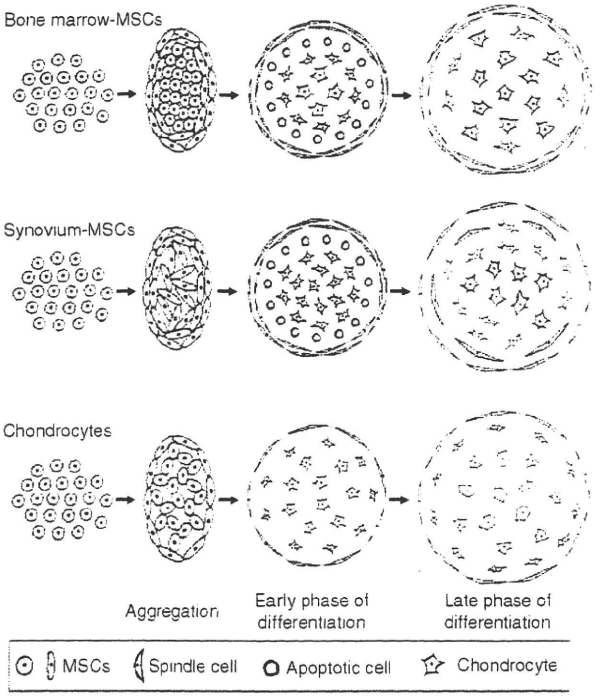

Figure 9 Scheme for morphological events during *in vitro* chondrogenesis of bone marrow-, synovium-MSCs, and chondrocytes. Explanations are summarized in Table 1.

mation could possibly clarify the cell source and the mechanisms of the ectopic cartilage formation.

The chondrogenic medium used in the study was previously demonstrated to be suitable for MSCs derived from bone marrow[16,18] and synovium.[23] This chondrogenic medium may not be optimal for chondrocytes. However, in this study, we demonstrated that colony-forming cells derived from cartilage produced cartilage matrix in the condition we used. If we had performed *in vitro* chondrogenesis of chondrocytes with a medium more suitable for chondrocytes, we could not have concluded that morphological differences are due to a different origin of the cells, because different culture medium may affect the morphology of the cells. Therefore, we used common chondrogenic medium for *in vitro* chondrogenesis of bone marrow-MSCs, synovium-MSCs, and chondrocytes.

There were some differences of histological patterns between toluidine blue and type II collagen staining, both of which were supposed to be correlated principally. We embedded histological samples in Epon for toluidine blue staining in order to enable detailed analysis, and in paraffin for immunohistology.[19] We did not use serial sections for toluidine blue and type II collagen staining, resulting in different patterns between in toluidine blue and type II collagen staining.

For treatment of cartilage defect, transplantation of MSCs is an effective strategy. Among a variety of MSC sources, bone marrow and synovium are useful for high chondrogenic potential of their MSCs. The two MSCs contain common features, but distinguishing properties dependent on their origin are emerging.[6–9,11,12] Colony-forming efficiency was higher in synovium-MSCs but colony size was larger in bone marrow-MSCs.[7] Expression of PDGF receptor-α was higher in synovium-MSCs based on flow cytometrical analysis.[12] In this study, we demonstrated morphological differences during *in vitro* chondrogenesis of bone marrow- and synovium-MSCs. Biologically, these differences are due to their different gene profiles. We previously compared gene profiles of bone

marrow- and synovium-MSCs. The expression levels of chitinase 3-like 1 (CHI3L1), aggrecan 1, WINT1-inducible signaling pathway protein 2 (WISP2), fibulin 1, and S100 calcium-binding protein were extremely low in bone marrow-MSCs and high in synovium-MSCs.[10]

Cytologically, differences of cell–cell junctions at the aggregation phase in the three populations were interesting. Wuchter *et al* recently reported novel type cell junctions. They demonstrated that bone marrow-MSCs under monolayer conditions were interconnected by special tentacle-like cytoplasmatic protrusions and invaginations.[24] Wagner and Ho[25] described that the frequency and morphology of these conjunction complexes were greatly affected by culture conditions. In our experiments, further detailed investigation would provide new insight into the nature of cell junctions in MSCs during the chondrogenesis.

Conclusions

In this study, we revealed morphological differences of bone marrow-MSCs, synovium-MSCs, and chondrocytes during *in vitro* chondrogenesis. The most obvious differences in the three populations were observed at the aggregation phase in the deep zone.

ACKNOWLEDGEMENTS

We thank Kenjiro Wake for valuable suggestions, Akiko Yokoyama for *in vitro* chondrogenesis of MSCs, Miyoko Ojima for histological analyses, and Yuko Kawamura for preparing the figures. This study was supported by grants from the Japan Society for the Promotion of Science (19500403) to SI, (21591937) to TM, (21591914) to IS, and the Japanese Ministry of Education (Global Center of Excellence (GCOE)) Program, International Research Center for Molecular Science in Tooth and Bone Diseases, Tokyo Medical and Dental University to TM.

DISCLOSURE/CONFLICT OF INTEREST

The authors declare no conflict of interest.

1. Koga H, Engebretsen L, Brinchmann JE, *et al.* Mesenchymal stem cell-based therapy for cartilage repair: a review. Knee Surg Sports Traumatol Arthrosc 2009;17:1289–1297.
2. Koga H, Shimaya M, Muneta T, *et al.* Local adherent technique for transplanting mesenchymal stem cells as a potential treatment of cartilage defect. Arthritis Res Ther 2008;10:R84.
3. Koga H, Muneta T, Ju YJ, *et al.* Synovial stem cells are regionally specified according to local microenvironments after implantation for cartilage regeneration. Stem Cells 2007;25:689–696.
4. Horie M, Sekiya I, Muneta T, *et al.* Intra-articular injected synovial stem cells differentiate into meniscal cells directly and promote meniscal regeneration without mobilization to distant organs in rat massive meniscal defect. Stem Cells 2009;27:878–887.
5. Sekiya I, Larson BL, Smith JR, *et al.* Expansion of human adult stem cells from bone marrow stroma: conditions that maximize the yields of early progenitors and evaluate their quality. Stem Cells 2002;20:530–541.
6. Koga H, Muneta T, Nagase T, *et al.* Comparison of mesenchymal tissues-derived stem cells for *in vivo* chondrogenesis: suitable conditions for cell therapy of cartilage defects in rabbit. Cell Tissue Res 2008;333:207–215.
7. Sakaguchi Y, Sekiya I, Yagishita K, *et al.* Comparison of human stem cells derived from various mesenchymal tissues: superiority of synovium as a cell source. Arthritis Rheum 2005;52:2521–2529.
8. Yoshimura H, Muneta T, Nimura A, *et al.* Comparison of rat mesenchymal stem cells derived from bone marrow, synovium, periosteum, adipose tissue, and muscle. Cell Tissue Res 2007;327:449–462.
9. Mochizuki T, Muneta T, Sakaguchi Y, *et al.* Higher chondrogenic potential of fibrous synovium- and adipose synovium-derived cells compared with subcutaneous fat-derived cells: distinguishing properties of mesenchymal stem cells in humans. Arthritis Rheum 2006;54:843–853.
10. Morito T, Muneta T, Hara K, *et al.* Synovial fluid-derived mesenchymal stem cells increase after intra-articular ligament injury in humans. Rheumatology (Oxford) 2008;47:1137–1143.
11. Segawa Y, Muneta T, Makino H, *et al.* Mesenchymal stem cells derived from synovium, meniscus, anterior cruciate ligament, and articular chondrocytes share similar gene expression profiles. J Orthop Res 2008;27:435–441.
12. Nimura A, Muneta T, Koga H, *et al.* Increased proliferation of human synovial mesenchymal stem cells with autologous human serum: comparisons with bone marrow mesenchymal stem cells and with fetal bovine serum. Arthritis Rheum 2008;58:501–510.
13. Saris DB, Vanlauwe J, Victor J, *et al.* Characterized chondrocyte implantation results in better structural repair when treating symptomatic cartilage defects of the knee in a randomized controlled trial versus microfracture. Am J Sports Med 2008;36:235–246.
14. Kirsch T. Determinants of pathological mineralization. Curr Opin Rheumatol 2006;18:174–180.
15. Nagase T, Muneta T, Ju YJ, *et al.* Analysis of the chondrogenic potential of human synovial stem cells according to harvest site and culture parameters in knees with medial compartment osteoarthritis. Arthritis Rheum 2008;58:1389–1398.
16. Sekiya I, Colter DC, Prockop DJ. BMP-6 enhances chondrogenesis in a subpopulation of human marrow stromal cells. Biochem Biophys Res Commun 2001;284:411–418.
17. Sekiya I, Vuoristo JT, Larson BL, *et al. In vitro* cartilage formation by human adult stem cells from bone marrow stroma defines the sequence of cellular and molecular events during chondrogenesis. Proc Natl Acad Sci USA 2002;99:4397–4402.
18. Sekiya I, Larson BL, Vuoristo JT, *et al.* Comparison of effect of BMP-2, -4, and -6 on *in vitro* cartilage formation of human adult stem cells from bone marrow stroma. Cell Tissue Res 2005;320:269–276.
19. Ichinose S, Tagami M, Muneta T, *et al.* Morphological examination during *in vitro* cartilage formation by human mesenchymal stem cells. Cell Tissue Res 2005;322:217–226.
20. Sakaguchi Y, Sekiya I, Yagishita K, *et al.* Suspended cells from trabecular bone by collagenase digestion become virtually identical to mesenchymal stem cells obtained from marrow aspirates. Blood 2004;104:2728–2735.
21. Sekiya I, Larson BL, Vuoristo JT, *et al.* Adipogenic differentiation of human adult stem cells from bone marrow stroma (MSCs). J Bone Miner Res 2004;19:256–264.
22. Tallheden T, Karlsson C, Brunner A, *et al.* Gene expression during redifferentiation of human articular chondrocytes. Osteoarthritis Cartilage 2004;12:525–535.
23. Shirasawa S, Sekiya I, Sakaguchi Y, *et al. In vitro* chondrogenesis of human synovium-derived mesenchymal stem cells: optimal condition and comparison with bone marrow-derived cells. J Cell Biochem 2006;97:84–97.
24. Wuchter P, Boda-Heggemann J, Straub BK, *et al.* Processus and recessus adhaerentes: giant adherens cell junction systems connect and attract human mesenchymal stem cells. Cell Tissue Res 2007;328:499–514.
25. Wagner W, Ho AD. Mesenchymal stem cell preparations—comparing apples and oranges. Stem Cell Rev 2007;3:239–248.

Osteoarthritis and Cartilage 18 (2010) 1300–1309

Osteoarthritis and Cartilage

Magnesium enhances adherence and cartilage formation of synovial mesenchymal stem cells through integrins

M. Shimaya †, T. Muneta †‡, S. Ichinose §, K. Tsuji ‡, I. Sekiya ‖*

† Section of Orthopedic Surgery, Graduate School, Tokyo Medical and Dental University, Tokyo, Japan
‡ Global Center of Excellence Program for International Research Center for Molecular Science in Tooth and Bone Disease, Tokyo Medical and Dental University, Tokyo, Japan
§ Instrumental Analysis Research Center, Tokyo Medical and Dental University, Tokyo, Japan
‖ Section of Cartilage Regeneration, Graduate School, Tokyo Medical and Dental University, Tokyo, Japan

ARTICLE INFO

Article history:
Received 23 December 2009
Accepted 10 June 2010

Keywords:
Magnesium
Mesenchymal stem cell
Integrin
Cartilage regeneration

SUMMARY

Objective: We previously reported that more than 60% of synovial mesenchymal stem cells (MSCs) placed on osteochondral defects adhered to the defect within 10 min and promoted cartilage regeneration. The efficiency of adherence is considered to depend on the interaction between cells and extracellular matrix (ECM), in which integrins may play some important roles. Divalent cations such as calcium, magnesium, and manganese may affect functions of integrins, and the integrins may be involved in differentiation of MSCs. Among divalent cations, magnesium is used in clinical practice as a therapeutic agent and increases the affinity of integrin to ECM. In this study, we investigated whether magnesium enhanced adherence and chondrogenesis of synovial MSC through integrins.

Methods: We performed assays for adherence of human synovial MSCs to collagen-coated slides, *in vitro* chondrogenesis, *ex vivo* assays for adherence of human synovial MSCs to osteochondral defect, and *in vivo* assays for adherence and cartilage formation of synovial MSCs in a rabbit osteochondral defect model.

Results: Magnesium increased adhesion of human synovial MSCs to collagen, and this effect was inhibited by neutralizing antibodies for integrin α3 and β1. Magnesium also promoted synthesis of cartilage matrix during *in vitro* chondrogenesis of synovial MSCs, which was diminished by neutralizing antibodies for integrin β1 but not for integrin α3. *Ex vivo* analyses demonstrated that magnesium enhanced adherence of human synovial MSCs to osteochondral defects. *In vivo* studies in rabbits showed that magnesium promoted adherence at 1 day and cartilage formation of synovial MSCs at 2 weeks.

Conclusion: Magnesium enhanced adherence of synovial MSCs through integrins, which promoted synthesis of cartilage matrix at an early phase.

Introduction

Mesenchymal stem cells (MSCs) are useful cell sources for regenerative medicine[1–3]. Synovium is a practical MSC source for cartilage regeneration because of its superior proliferation potential with autologous human serum and high chondrogenic ability[4–10]. Current cell therapy for cartilage regeneration requires invasive procedures, periosteal coverage, and the use of scaffold[11,12]. We recently reported that more than 60% of synovial MSCs suspended in phosphate buffered saline (PBS) placed on the osteochondral defect adhered to the defect in 10 min and promoted cartilage regeneration[13]. This method makes it possible to transplant synovial MSCs on the osteochondral defect arthroscopically; however, any improvement in its efficiency for cell adhesion remains in question.

Integrins are a family of cell surface molecules which mediate adhesive interaction with extracellular matrix (ECM), activate intracellular pathways, and play important roles in many biological processes including differentiation[14–16]. Some functions of integrins are dependent on interaction with divalent cations such as calcium, magnesium, and manganese through a metal ion dependent adhesion site (MIDAS) and MIDAS-like motives[17,18]. Among divalent cations, calcium and magnesium are widely used in clinical practices as therapeutic agents, and magnesium increases the affinity of integrins for ligands including ECM in a millimolar concentration[19], while calcium reverses the increased affinity in some cases[20].

* Address correspondence and reprint requests to: Ichiro Sekiya, Tokyo Medical and Dental University, Graduate School, Section of Cartilage Regeneration, 1-5-45 Yushima, Bunkyo-ku, Tokyo, 113-8519 Japan. Tel: 81-3-5803-4020; Fax: 81-3-5803-0266.
E-mail addresses: shimaya.orj@tmd.ac.jp (M. Shimaya), muneta.orj@tmd.ac.jp (T. Muneta), ichinose.bioa@tmd.ac.jp (S. Ichinose), ktsuji.gcoe@tmd.ac.jp (K. Tsuji), sekiya.orj@tmd.ac.jp (I. Sekiya).

1063-4584/$ – see front matter © 2010 Osteoarthritis Research Society International. Published by Elsevier Ltd. All rights reserved.
doi:10.1016/j.joca.2010.06.005

We hypothesized that the addition of magnesium to MSC suspension might enhance adherence of synovial MSCs to osteochondral defect, increase cartilage matrix synthesis of synovial MSCs, and finally accelerate cartilage regeneration. The purpose of this study was to investigate the effect of magnesium on adherence and cartilage formation of synovial stem cells through integrins. The results will clarify some novel functions of integrins and provide some clues for obtaining better clinical outcome for cartilage regeneration with synovial MSCs.

Materials and methods

Isolation and culture of MSCs

The study was approved by an institutional review board, and informed consents were obtained from all subjects. Human synovium harvested from three donors (27 and 34-year-old males and a 28-year-old female) during arthroscopic surgery was digested with 3 mg/ml Collagenase D (Roche Diagnostics, Mannheim, Germany) for 3 h. The nucleated cells were cultured at a clonal density in 150 cm^2 culture dishes (Nalge Nunc International, Rochester, NY) in 20 ml α-minimum essential medium (MEM) (Invitrogen, Carlsbad, CA) containing 10% fetal bovine serum (FBS) (Invitrogen) for 14 days, then replated at 50 cells/cm^2, cultured for 14 days, and cryopreserved. The frozen cells were slowly thawed, plated, and incubated for 4 days. The cells were replated at 50 cells/cm^2 again and cultured for 14 days for analyses.

Skeletally mature Japanese white rabbits weighing 3.0 kg on average were used. Animal care was in accordance with our institutional guidelines. Synovium harvested from the right knees under anesthesia was digested in a 3 mg/ml collagenase type V (Sigma Aldrich, St. Louis, MO) solution for 3 h. After filtering, the nucleated cells were cultured at 3×10^6 cells/cm^2 for 7 days, replated at 50 cells/cm^2, and cultured for 14 days for analyses.

Cell differentiation

One hundred human synovial MSCs were plated in 60-cm^2 dishes and cultured for 2 weeks. For adipogenesis, the medium was changed to adipogenic medium. The cells were cultured for an additional 3 weeks and stained with Oil red O solution. For osteogenesis, the medium was changed to osteogenic medium. The cells were cultured for an additional 4 weeks and stained with alizarin red solution[4,8]. For *in vitro* chondrogenic differentiation, 300,000 human synovial MSCs were pelleted and cultured for 7 and 21 days in chondrogenic medium containing 500 ng/ml bone morphogenetic protein (BMP)-7, (Stryker Biotech, Boston, MA), 10 ng/ml transforming growth factor (TGF)β3 (R&D Systems, Minneapolis, MN), and 100 nM dexamethasone (Sigma–Aldrich). The concentration of magnesium was adjusted by adding $MgCl_2$. For analyses of involvement of integrins, the cells were pre-incubated with or without 20 μg/ml neutralizing antibodies for integrin β1 (P5D2, R&D Systems) or α3 (P1B5, Santa Cruz Biotechnology, Santa Cruz, CA) for 1 h, then the cells were pelleted and cultured in chondrogenic medium containing 0.8 or 5 mM magnesium for 21 days. No antibodies were re-added during the culture.

Surface epitopes

One hundred thousand synovial MSCs suspended in 200 μl PBS containing 20 μg/ml of antibody were incubated for 20 min at 4°C and subsequently incubated with R-phycoerythrin-coupled anti mouse IgG (AbD Serotech, Oxford, UK) for 20 min. Antibodies used in neutralizing against integrin β1 (P5D2, R&D Systems), α3 (P1B5, Santa Cruz Biotechnology), α4 (HP2/1, AbD Serotech), α5 (JBC5, AbD Serotech) and isotype control (R&D Systems) were used to detect epitopes. FITC conjugated antibody for the integrin α2 (AK7, AbD Serotech), CD44 and CD106 (eBioscience, San Diego, CA); CD105 and CD166 (Ancell corporation, Bayport, MN), CD45, CD34, CD90 and isotype control (Becton Dickinson, Franklin Lakes, NJ) were used. In double-staining for integrin α2 and α3, phycoerythrin (PE)-conjugated antibody for integrin α3 (BioLegend, San Diego, CA) was used.

In vitro *cell adhesion assay*

One hundred thousand human synovial MSCs suspended in 10 μl PBS with 0, 0.1, 1, 5, and 10 mM magnesium were placed on 8-well culture slides with or without type I collagen coating (Becton-Dickinson) for 10 min. After washing slides with PBS, the number of cells in 4 high power fields (HPFs) was counted, and the mean was determined. For neutralizing against adhesion molecules, cells were pre-incubated in PBS 20 μg/ml antibody for integrin β1 (P5D2, R&D Systems), vascular adhesion molecule 1 (VCAM-1; BBIG-V1, R&D Systems), activated leukocyte-cell adhesion molecule (ALCAM; 105901, R&D Systems), integrin α2 (P1E6, Abcam, Cambridge, UK), α3 (P1B5, Santa Cruz Biotechnology), α4 (HP2/1, AbD Serotech), α5 (JBC5, AbD Serotech) and isotype control (R&D Systems) for 1 h.

Immunocytochemical analysis

Ten thousand human synovial MSCs adhering to collagen-coat slides under 10 mM magnesium were fixed with 99.5% acetone for 15 min. The slides were stained with the integrin α2 (P1E6, Abcam) or α3 (P1B5, Santa Cruz Biotechnology) (1:1000) for 1 h. After washing, the slides were stained with goat anti-mouse IgG labeled with Alexa fluor 488 (Invitrogen) for 1 h. The nuclei were stained with Hoechst 33342 (Invitrogen). The number of integrin-positive cells and nuclei was counted using 3 HPFs.

Assay for sulfated glycosaminoglycan (sGAG) content of pellets

After 21 days of culture, pellets were digested for 24 h at 60°C in papain buffer (200 μg/ml papain (Sigma–Aldrich) and dissolved in 50 mM phosphate buffer containing 1 M NaCl, 5 mM cysteine–HCl and 1 mM EDTA). The GAG concentration of supernatant was determined by the Blyscan-assay (Biocolor Ltd, Newtonabbay, Ireland) according to manufacturer's instructions.

Real-time polymerase chain reaction (PCR) analysis

Total RNA was extracted from the pellets cultured for 3 weeks using QIAzol (Qiagen, Hiden, Germany) and the RNeasy micro kit (Qiagen). cDNA was synthesized with oligo-dT primer from total RNA using the Transcriptor High Fidelity cDNA Synthesis kit (Roche Diagnostics) according to the manufacturer's protocol. Reverse transcription (RT) was performed by 30 min incubation at 55°C, followed by 5 min incubation at 85°C. Real-time PCR was performed in a LightCycler 480 instrument (Roche Diagnostics) using FastStart TaqMan Probe Master and TaqMan probes for COL2A1 (#75) and β-Actin (#64) (Roche Diagnostics). After an initial denaturation step (95°C for 10 min), amplification was performed for 40 cycles (95°C for 15 s, 60°C for 60 s).

DNA content of pellets

Undifferentiated MSCs and pellets at 21 days were digested with 3 mg/ml collagenase, and DNA was prepared with a QIAamp DNA mini kit (Qiagen). The DNA content was calculated from the absorbance at 260 nm.

Ex vivo *analyses of cells adhered to osteochondral defect*

Human osteochondral fragments at the lateral femoral condyle were harvested during total knee arthroplasty, and osteochondral defects at 2.5 mm in diameter were created. Then the defects were filled with 1.5×10^5 synovial MSCs labeled with DiI (Molecular Probes, Eugene, OR) in 8 μl PBS with 0, 1, and 10 mM magnesium. After 10 min, the fragments were turned over for 10 min. The DiI-positive cells in the dish were counted after trypsinization, and the number of the cells attached to the defects was calculated. The fluorescence images of the entire defect were photographed. The total fluorescence intensity of the remaining cells in the defect was determined by measuring the brightness in the defect using Image J software (National Institutes of Health, Bethesda, MD).

In vivo *analyses for adherence and cartilage formation*

Knees of rabbits were approached medially under anesthesia. Osteochondral defects (5 × 5 mm, 1.5 mm deep) were created in the trochlear groove. To transplant cells, the defect was filled with synovial MSCs suspension, and the knees were held stationary for 10 min with the defect facing upward. For adhesion analyses at 1 day, 2×10^6 allogenic DiI-labeled cells at passage 1 suspended in 30 μl PBS with 5 mM magnesium or in PBS in the contralateral knee were used. Total fluorescence intensity over the defect was evaluated by measuring the brightness of the entire defect using Image J software. The ratio of the fluorescence positive area over the defect was evaluated by measuring the square measure of the entire defect and the fluorescence positive area at 1 day. For analyses of cartilage regeneration at 14 and 28 days, 5×10^6 autologous synovial MSCs at passage 0, suspended in PBS with or without 5 mM magnesium were transplanted in the left knee 7 days after harvest of synovium from the right knee.

Histological analyses

The specimens were fixed with 4% paraformaldehyde solution, decalcified, and embedded in paraffin. Sections were stained with safranin-o/fast green. Image J was used for measurement of defects and safranin-o positive areas. Sections without staining were used for fluorescence.

For immunohistochemistry, sections were treated with 0.4 mg/ml proteinase K (DAKO, Carpinteria, CA) in Tris–HCl and normal horse serum after deparaffinization. Primary antibodies for type II collagen (Daiichi Fine Chemical, Toyama, Japan) and a secondary antibody of biotinylated horse anti-mouse IgG (Vector Laboratories, Burlingame, CA) were employed. Immunostaining was detected with VECTASTAIN ABC reagent (Vector Laboratories) followed by 3,3′-diaminobenzidine staining.

Transmission electron microscopy

Cartilage pellets and regenerated cartilage were fixed with 2.5% glutaraldehyde and post-fixed with 1% OsO_4. After dehydration, they were embedded in Epon 812. Ultrathin (90 nm) sections were collected on copper grids, double-stained with uranyl acetate and lead citrate, and then examined by transmission electron microscopy (H-7100, Hitachi, Hitachinaka, Japan)[18].

Immunoelectron microscopy

After fixation in 4% paraformaldehyde and 0.1% glutaraldehyde, pellets were immersed in 2.3 M sucrose for 24 h and frozen in liquid nitrogen. The frozen sections mounted on silane-coated glass were placed on droplets of 1% BSA on a Parafilm sheet and subsequently transferred to droplets of mouse antibody against collagen type I, type II (diluted to 1:20, Fuji Yakuhin, Japan) and chondroitin sulfate-proteoglycans (diluted to 1:50, Seikagaku Kogyo, Japan) for 48 h. They were then incubated with goat anti-mouse IgG + IgM conjugated with 10–15 nmΦ gold colloidal particles (diluted to 1:50 with 1% BSA in 0.1 M PBS, British Bio Cell International, UK) for 24 h. The sections were fixed in 2.5% glutaraldehyde, post-fixed in a 1% OsO_4 solution, and dehydrated in a graded series of ethanol. Then they were embedded in Epon 812, stained with uranyl acetate, and examined by TEM[21].

Statistical analyses

Mann–Whitney *U* tests were used. A value of $P < 0.05$ was considered significant.

Results

Magnesium increases adhesion of human synovial MSCs through integrin α3 and β1

Human synovial cells had a colony forming ability and multi-differentiation potentials [Fig. 1(A)]. Flow cytometric analyses demonstrated that human synovial cells expressed CD44, 90, 105, 166 highly, and CD34, 45, 106 at a low level [Fig. 1(B)]. These findings demonstrated that human synovial cells had characteristics similar to those of MSCs.

Magnesium increased the number of synovial MSCs attached to collagen-coated slides dose-dependently [Fig. 1(C)]. Time lapse analysis showed that 5 mM magnesium caused thinning of cell shape and spread the cells on collagen-coated slides within 5 min, while the cell was still thick and round even after 25 min without magnesium or collagen-coating [Fig. 1(D)]. Human MSCs also expressed integrin α5, β1 highly, integrin α2, α3 modestly, and integrin α4 at a low level [Fig. 1(B)]. The effect of magnesium on attachment of synovial MSCs was diminished by the neutralizing antibodies for integrin α3 and β1 [Fig. 1(E)]. Some studies have reported that α2 integrin was a collagen receptor[14,15], therefore, we attempted more detailed examinations of antibodies for integrin α2 and α3. Double staining flow cytometric assay showed that the double positive rate was only 17% [Fig. 1(F)]. Immunocytochemical analysis showed that the α2 positive cell rate was 38%, and the α3 positive cell rate was 73% among cells adhering to the collagen slide in the presence of 10 mM magnesium [Fig. 1(G)].

Magnesium enhances chondrogenesis of human synovial MSCs

In pellet culture for *in vitro* chondrogenesis, the weight of the pellets at 7 days was affected by magnesium concentration, and 5 mM magnesium had the greatest effect [Fig. 2(A)]. The weight of the pellets cultured in 5 mM magnesium for 21 days was also heavier than those cultured in 0.8 mM magnesium in three other donors [Fig. 2(B left)]. Pellets cultured in 5 mM magnesium produced more sGAG than pellets cultured in 0.8 mM magnesium [Fig. 2(B, right)].

Pretreatment with neutralizing antibody for integrin β1 resulted in a decrease of pellet weight, sGAG content and safranin-o staining in pellets cultured in 5 mM magnesium at 21 days [Fig. 2(C)]. Pellets cultured in 5 mM magnesium showed higher COL2A1 expression than pellets cultured in 0.8 mM magnesium [Fig. 2(D)]. The DNA content of pellets greatly decreased in 3 weeks, and no significant difference was observed between pellets cultured in 0.8 and 5 mM magnesium [Fig. 2(E)].

Transmission electron microscopy revealed polygonal cells with short processes, containing well-developed rough

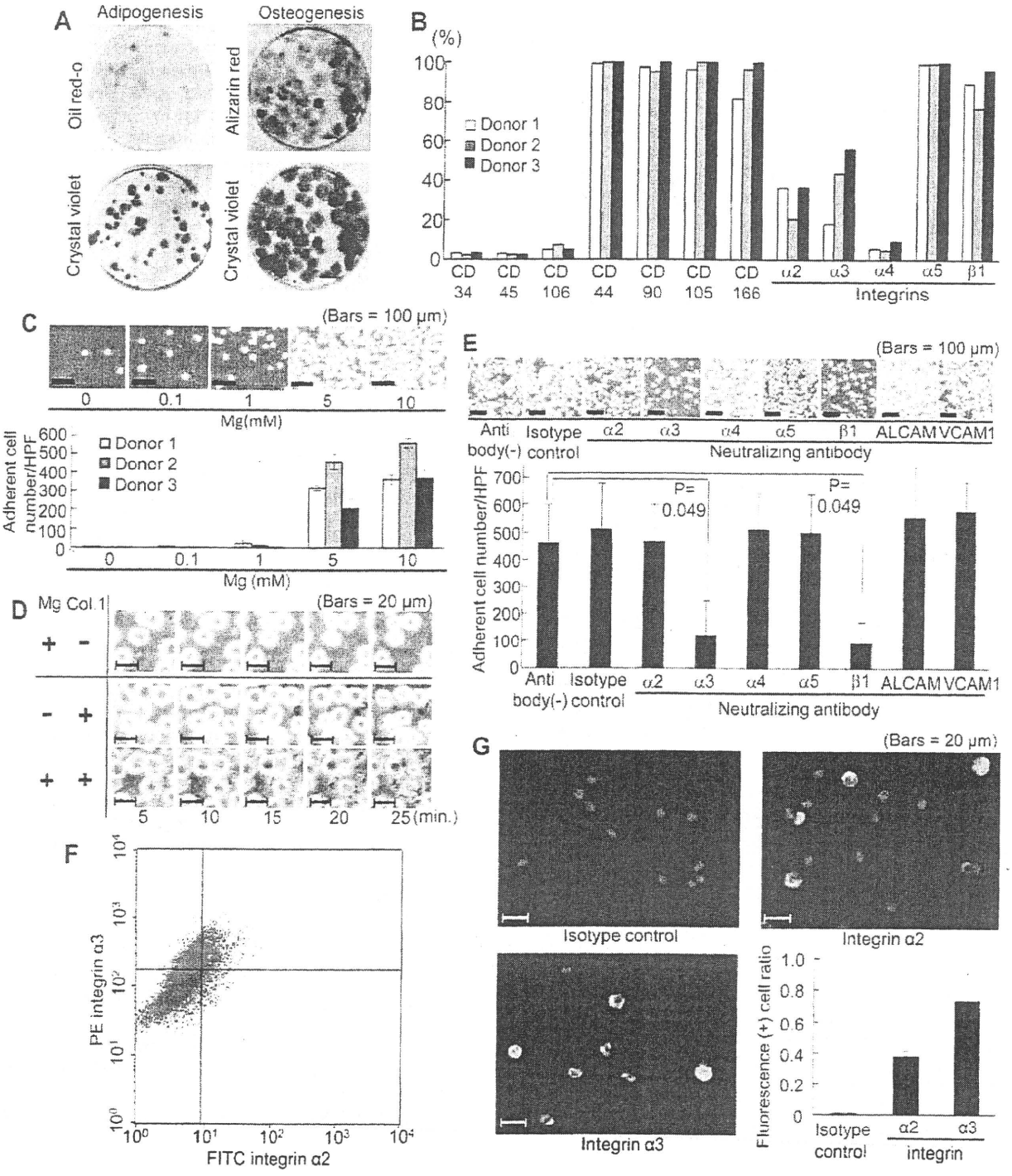

Fig. 1. Properties of human synovial MSCs and magnesium effects on adherence. (A) Macroscopic images of adipogenic and osteogenic differentiation of colony forming cells. (B) Surface epitopes. (C) Microscopic images and quantification of adherent cells on collagen-coated slides at indicated concentrations of magnesium. Values are means with 95% confidence interval (CI) ($n = 3$). (D) Time-lapse analyses of cell morphology during their adhesion on collagen coated slides with or without magnesium. (E) Microscopic images and quantification of adherent cells pretreated with neutralizing antibodies. Values are means with 95% CI ($n = 3$). (F) Two-dimensional plotting for integrin α2 and α3 (red), and for the isotype controls (blue). (G) Immunocytochemical analysis for integrin α2 and α3 of adhering cells on collagen-coated slides in the presence of 10 mM magnesium. The number of positive cells (green) and nuclei (blue) was counted using 3 HPFs, and the integrin positive ratio was calculated. Values are means with 95% CI ($n = 3$).

endoplasmic reticulum (rER), and surrounded by thin, faintly striated collagen fibrils in pellets cultured for 21 days even in 0.8 mM magnesium. Thick collagen bundles consisting of a large number of parallel collagen fibers characteristic for fibrocartilage[22,23] could not be seen [Fig. 2(F, upper panels)]. Immunoelectron microscopic analysis demonstrated expressions of type II collagen, chondroitin sulfate, and the absence of type I collagen in ECM [Fig. 2(F, lower panels)]. These results indicate that pellets of synovial MSCs differentiated into hyaline cartilage.

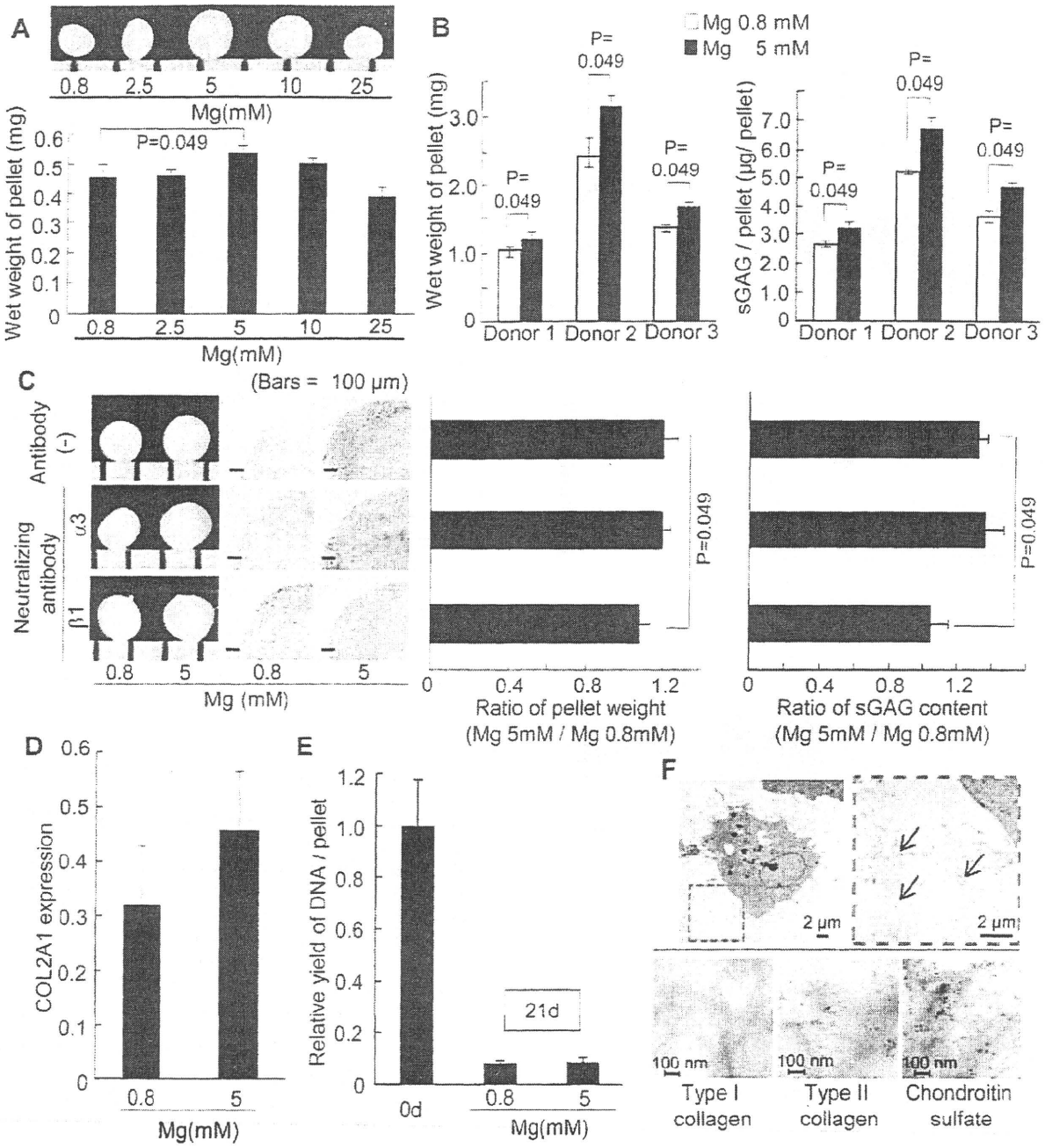

Fig. 2. Magnesium effects on *in vitro* chondrogenesis of human synovial MSCs. (A) Pellet cultured in chondrogenic medium at indicated concentration of magnesium. Macroscopic images at 1 week (upper, scale = 1 mm) and quantification of wet weight of pellets at 1 week (lower). Values are means with 95% CI for three pellets from one donor. (B) Wet weight (left) and sGAG content (right) of pellets cultured for 21 days in 0.8 and 5 mM magnesium. Values are means with 95% CI for three pellets from each donor. (C) Pellets of MSCs pretreated with antibodies. Pretreated pellets were cultured in chondrogenic medium at 0.8 and 5 mM magnesium for 21 days. Macroscopic images with 1 mm scale (left), histologies stained with safranin-o (middle), and relative weight and sGAG content of pellets cultured in 5 mM magnesium to those cultured in 0.8 mM magnesium (right). Values are means with 95% CI ($n = 3$). (D) Real time PCR analysis for gene expression of Col2A1 in pellets cultured for 21 days in 0.8 or 5 mM magnesium. β-Actin was used as an internal control. Values are means with 95% CI ($n = 3$). (E) DNA content of pellets at day 0 and day 21. Values are means with 95% CI ($n = 3$). (F) Transmission electron microscopic image (upper left), the magnified image (upper right) and immunoelectron microscopic images (lower) of pellets cultured for 21 days in chondrogenic medium containing 0.8 mM magnesium. The arrows indicate collagen fibrils (upper right).

Magnesium promotes adherence of human synovial MSCs on osteochondral defects in vitro

Macroscopic and fluorescence observations indicated that DiI labeled MSCs in the defect increased along with magnesium concentration. The intensity of DiI fluorescence of MSCs suspended in 10 mM magnesium was significantly higher than that in PBS without magnesium [Fig. 3(A)]. Histological analyses also indicated an increase of DiI-labeled cells in the defect along with magnesium concentration, and that the number of adherent MSCs in 10 mM magnesium was significantly higher than that in PBS without magnesium [Fig. 3(B)]. The fluorescence intensity of the defects significantly decreased with antibodies for integrin α3 or β1 [Fig. 3(C)].

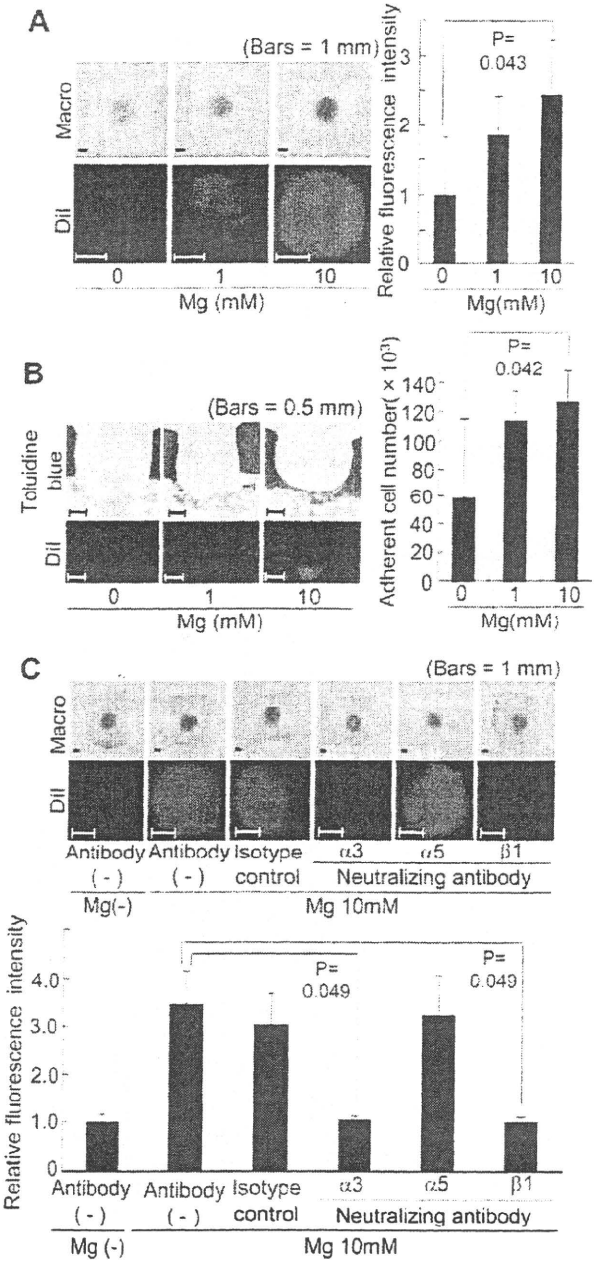

Fig. 3. *Ex vivo* studies for magnesium effects on adherence of human synovial MSCs on osteochondral defects. (A) Top side view of the osteochondral defects without fluorescence (left upper), with fluorescence (left lower), and quantification of the relative fluorescence intensity of DiI labeled MSCs in the defects (right). Values are means with 95% CI. Four pieces of osteochondral fragments were used for each group. (B) Histological analyses and quantification of attached cell number. Toluidine blue staining (left upper), the fluorescence image for DiI (left lower), and quantification of adherent cell number (right). Values are means with 95% CI. Four pieces of osteochondral fragments were used for each group. (C) Effects of the neutralizing antibodies. Top side view of the defects without fluorescence (upper) and with fluorescence (middle). The relative fluorescence intensities of cells in the defects were quantified (lower). Values are means with 95% CI. Three pieces of osteochondral fragments were used for each group.

Magnesium enhances adherence of rabbit synovial MSCs in osteochondral defects in vivo

Osteochondral defects in the rabbit knee joint were filled with DiI-labeled MSCs suspended in PBS with or without 5 mM magnesium, held stationary for 10 min [Fig. 4(A)], and then the joint capsule was closed. Under fluorescence at day 1, the DiI positive area was more distinct [Fig. 4(B, upper panels)], and the fluorescence intensity of defects [Fig. 4(B, lower left)] and the ratio of fluorescence positive area over the defect [Fig 4(B, lower right)] were significantly greater in the defect treated with magnesium. Histologically, a greater number of DiI-positive cells adhered to the defect treated with magnesium. Furthermore, a greater number of cells accumulated on the layer of cells which are attached to the basement of defects in the presence of magnesium [Fig. 4(C)].

Addition of magnesium results in a greater amount of cartilage matrix by MSCs in vivo

At 2 weeks, cartilage matrix stained with safranin-o appeared more distinct in the osteochondral defect treated with synovial MSCs suspended with magnesium than in the defect treated with synovial MSCs suspended without magnesium [Fig. 5(A)]. The safranin-o positive area ratio was significantly higher in the defect treated with magnesium [Fig. 5(B)]. At 4 weeks, the amount of cartilage matrix increased, and the difference of the ratio of the safranin-o positive area to the defect area lessened in both groups. The matrix of regenerated cartilage was positive for type II collagen in both groups [Fig. 5(C)]. Regenerated cartilage consisted of polygonal cells containing well-developed rER, with short processes, and surrounded with thin, faintly striated collagen fibrils [Fig. 5(D)]. These results indicate that the osteochondral defect was regenerated with hyaline cartilage.

Discussion

MSCs are defined as having been derived from mesenchymal tissue and by their functional capacity to self-renew and to generate a number of differentiated progeny[1,10]. Since the earliest studies by Friedenstein *et al.*, the standard assay used to identify the self-renewal ability of MSCs is the colony forming unit fibroblast assay[24]. Although clonal colonies of MSCs are readily prepared, they rapidly become heterogeneous as they expand[9,25,26]. We collected bulk colony-forming cells, and the cells used in the present study showed both colony-forming ability and multipotentiality. Surface markers were also identical to those of MSCs published elsewhere[1,4,7–10]. Therefore, the synovial cells we used were defined as MSCs, though the cells were not clonal. This point should be considered when our study is discussed in the field of "stem cells".

It was reported that magnesium enhanced adhesion of some tumor cells or lineage cell lines to collagen and fibronectin coated slides. Grzesiak *et al.* demonstrated that human fibroblast WI38 bound to type I collagen under regulation by shift in the concentrations of extracellular divalent cations. In their report, cells adhered to collagen more effectively along with the concentration of magnesium through integrins[20]. However, there have been no reports demonstrating that magnesium enhanced adhesion of MSCs to collagen coated slides or osteochondral defects. Furthermore, improvement of the efficiency of attachment of stem cells is currently one of the topics for stem cell biology and regenerative medicine. An increase in adherence of cells leads to the improvement of "efficiency of transplantation," a factor of increasing interest in cell based regenerative medicine[27]. We believe that this paper contributes greatly to the field of cell therapy for regenerative medicine.

Although Pittenger *et al.* reported that bone marrow MSCs expressed integrins α1, α2, α3, and β1, integrins expressed in human synovial MSCs have not been reported[1]. In this study, surface epitope analyses revealed that synovial MSCs expressed integrin α5 and β1 highly, and α2 and α3 moderately.

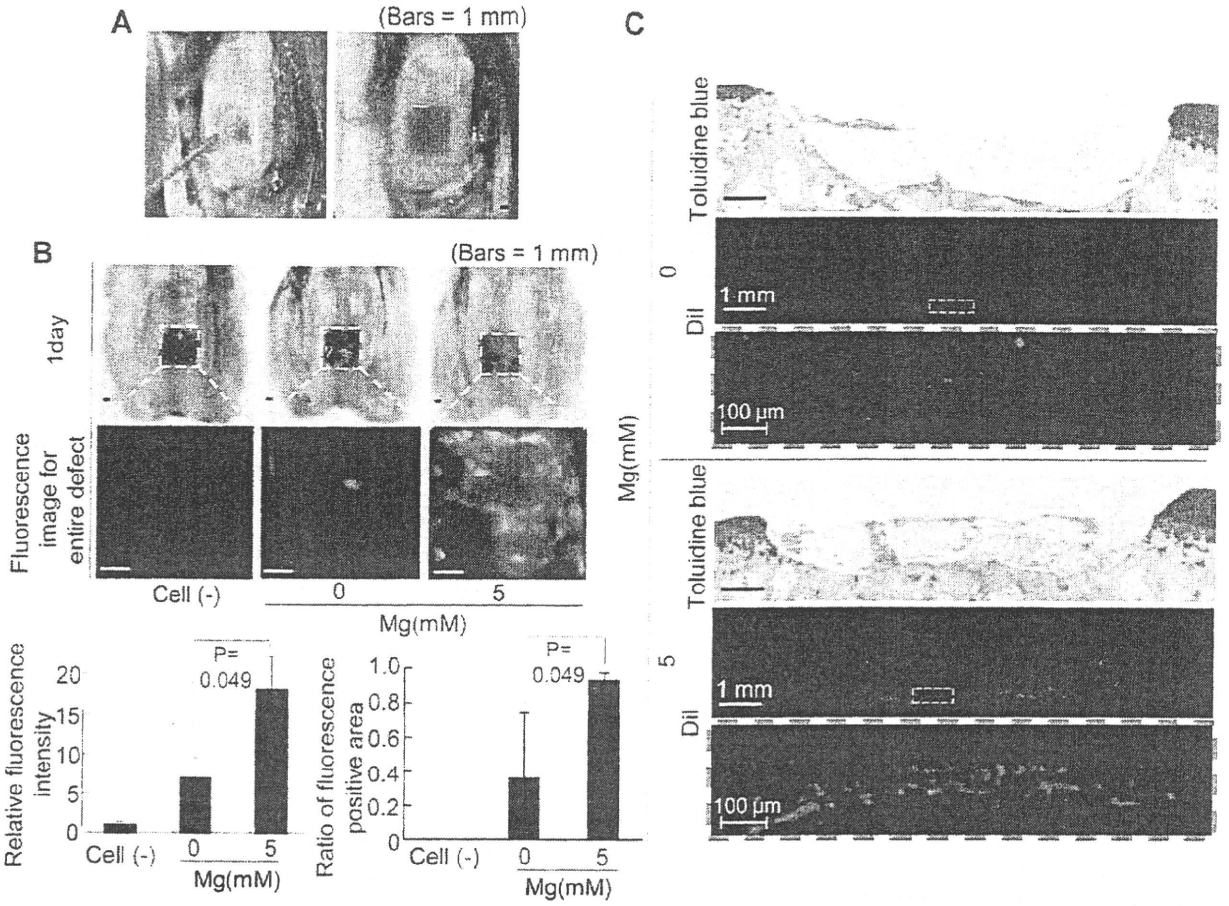

Fig. 4. *In vivo* analyses for magnesium effects on adherence of rabbit synovial MSCs on osteochondral defects. (A) Procedure for cell transplantation. Osteochondral defect was created, and needle was prepared over the defect (left). Cell suspension was dripped onto the defect, and this position was kept for 10 min (right). (B) Macroscopic and macroscopic fluorescence images of the defect for DiI labeled MSCs (upper six panels), quantification of relative fluorescence intensity over the defect at 1 day (lower left) and the ratio of fluorescence positive area over the defect at 1 day (lower right). The ratio was evaluated by measuring the square measure of the entire defect and the fluorescence positive area within the defect. Values are means with 95% CI ($n = 3$). (C) Sagittal sections of histologies stained with toluidine blue (upper), for DiI (middle) and the magnified image (lower).

Previous reports indicated that integrin α3β1 was a promiscuous cell adherent receptor. Wayner *et al.* first identified Integrin α3β1 as a receptor for type I, and IV collagen, laminin, and fibronectin[28]. Berdichevsky *et al.* reported that antibody for integrin α3 inhibited adhesion to polymerized collagen in mammary epithelial cells[29]. Carter *et al.* reported that human keratinocytes cultured on fibronectin, collagen, or laminin were detached from cover slips in the presence of anti integrin α3 antibody[30]. Though integrin α2β1 is also considered as one of the collagen receptors[14,15], our results demonstrated that neutralizing antibodies for α3 and β1 inhibited adhesion of synovial MSCs on collagen-coated slides. This indicates that integrin α3β1 functions as an adherence factor of synovial MSCs to type I collagen-coated slides under a higher concentration of magnesium.

In this study, we evaluated *in vitro* chondrogenesis potential as pellet weight. We intensively investigated pellet culture of MSCs. During *in vitro* chondrogenesis of MSCs, the pellets increased in size and weight. Conversely, the DNA yield per pellet decreased. The radioactivity per DNA in the cells, assessed by prelabeling with 3H-thymidine, was stable during *in vitro* chondrogenesis of MSCs. The increase in pellet size can be attributed to production of ECM and not to the proliferation of the cells[5,31]. Pellet weight is always correlated with expressions of cartilage related mRNAs such as COL2A1, aggrecan, link protein, SOX5, SOX6, and SOX9. Pellet weight is also correlated with proteoglycan staining by safranin-o, type II collagen by immunostaining, protein expressions of chondroitin 4-sulfate, chondrotitin 6-sulfate, and hyaluronan by ELISA as we previously reported[4–9,25,32]. All the results demonstrate that the weights of the pellets are quantitative indicators for chondrogenesis of MSCs.

While magnesium did not affect the DNA content of pellets, magnesium increased the wet weight, sGAG content, and gene expression for type II collagen of pellets. The effect was significantly diminished after pretreatment with neutralizing antibody for integrin β1 without re-adding antibodies. We investigated sequential gene expression profiles of MSCs during *in vitro* chondrogenesis within 24 h, and a large number of gene expressions were dramatically altered within a few hours (data not shown). Also, our morphological analysis demonstrated that the ultrastructure was altered most dramatically within 1 day[21]. We speculated the effect of neutralizing antibody for integrin β1 as follows: The neutralizing antibody for β1 integrin affected *in vitro* chondrogenesis at an early period, and this influence remained at a later stage, resulting in a difference of synthesis of cartilage matrix. We examined the magnesium effect on adherence of rabbit synovial MSCs on osteochondral defects *in vivo*. DiI-labeled MSCs suspended in PBS with or without 5 mM magnesium were placed on the defects for 10 min, and then the rabbit was allowed to move freely after operation. The distributions of DiI positive MSCs in the defects at 1 day were less homogenous compared with the results of *ex vivo*

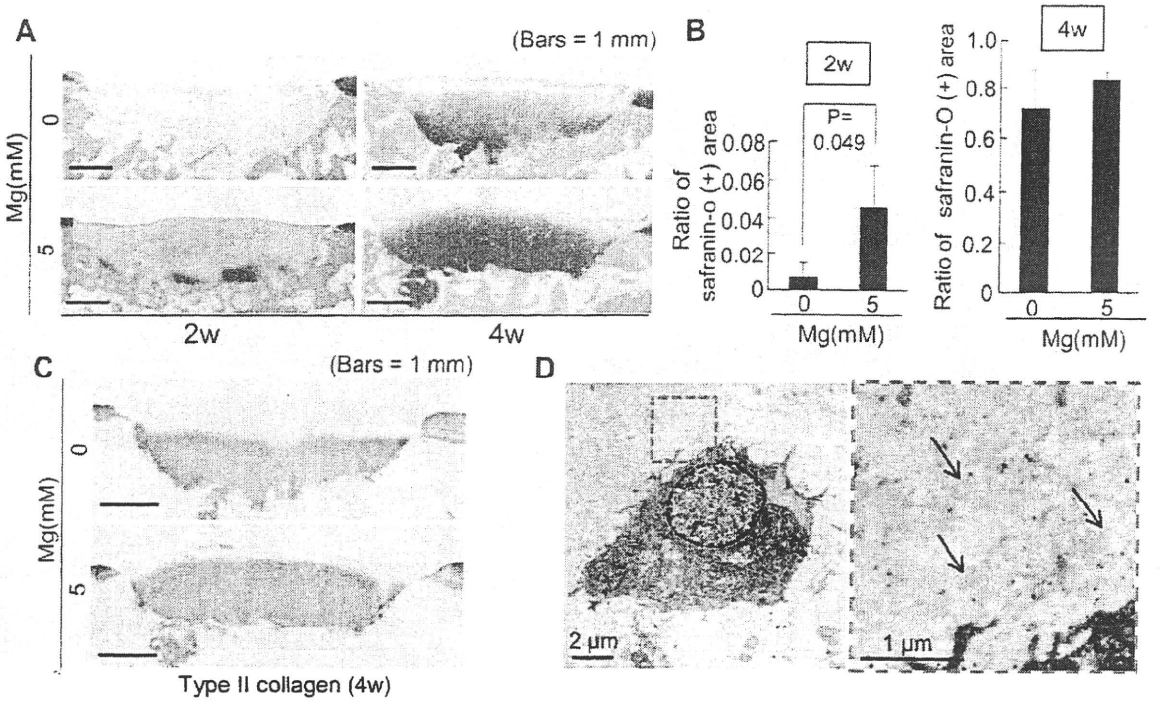

Fig. 5. *In vivo* analyses for magnesium effects on cartilage regeneration with rabbit synovial MSCs. (A) Sagittal section of defects stained with safranin-o at 2 and 4 weeks. (B) Ratio of safranin-o positive area to the total defect area at 2 and 4 weeks. Values are means with 95% CI ($n = 3$). (C) Immunohistochemistry for type II collagen at 4 weeks. (D) Transmission electron microscopic image of cell in regenerated cartilage of rabbit treated with synovial MSCs suspended in PBS at 4 weeks (left) and the magnified image (right). The arrows indicate collagen fibrils.

analysis. Intra-articular circumstance caused a discomfort condition for MSCs to continue in their attachment to osteochondral defects due to gravity force, bleeding, inflammatory reactions, and mechanical stresses accompanied with joint motions.

During *in vivo* situation, magnesium increased adherence of MSCs to the basement of the defect. Histologically, a greater number of cells accumulated on the layer of cells which were attached to the basement of the defects in the presence of magnesium. There are two possibilities to account for the result. Magnesium also may enhance accumulation of MSCs on the layer of the cells. Otherwise, a greater number of single-layered cells on the basement of defect may enhance accumulation of MSCs dependent on or independent of magnesium.

In vivo studies showed that cartilage matrix was regenerated earlier in the defects treated in the presence of 5 mM magnesium at 2 weeks. The number of cells involved in regeneration of cartilage is an important factor[33]. The difference of initial cell number attached to the defect or initial magnesium concentration may have been an

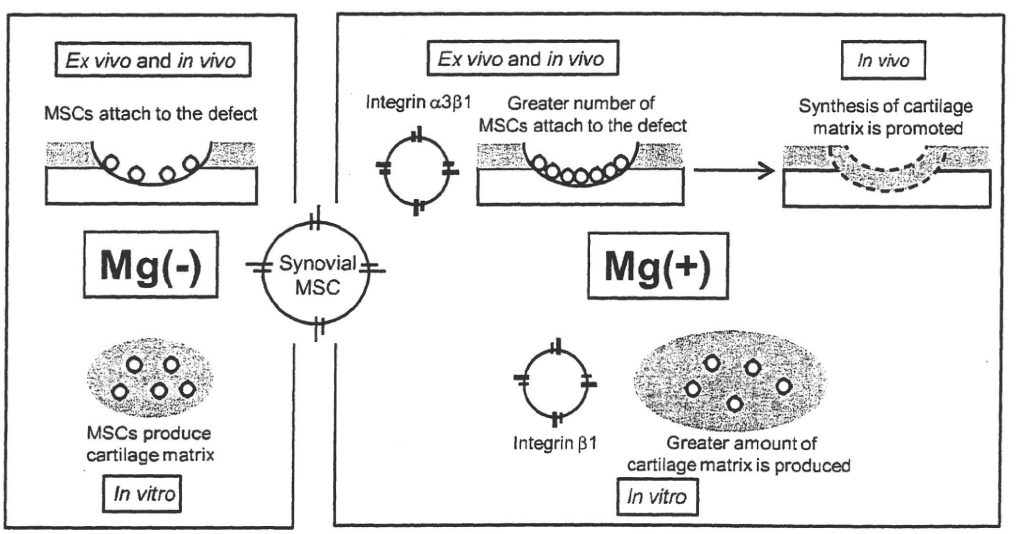

Fig. 6. Scheme of MSC based cartilage regeneration with magnesium. Magnesium increases MSC attachment and cartilage matrix formation through integrins at initial stage without toxicity.

influencing factor even after 2 weeks. As a whole, the presence of magnesium in cell suspension promoted cell adhesion to osteochondral defects and exerted no toxic effect on *in vivo* cartilage formation.

Standard media for cell culture, which also promote cell attachment, are not usually approved for clinical use. The most popular standard solution for clinical use is a lactate Ringer's solution, which does not contain magnesium. To demonstrate the effect of magnesium experimentally, we selected PBS (−), which is a more simplified standard solution close to a lactate Ringer's solution. PBS (+) contains 0.8 mM magnesium, and we showed that 5 mM magnesium had stronger effects for attachment and cartilage formation of synovial MSCs than PBS (+) containing 0.8 mM magnesium. Even if we had used PBS (+) as a control, the results would not have been significantly affected.

In summary, magnesium enhanced attachment of synovial MSCs to osteochondral defect through integrin α3β1. A greater number of MSCs were attached to the defect and promoted synthesis of cartilage matrix at an early phase. Furthermore, magnesium increased cartilage matrix synthesis through integrin β1 during *in vitro* chondrogenesis of synovial MSCs (Fig. 6).

Contributions

Masayuki Shimaya: conception and design, analysis and interpretation of the data, collection and assembly of data, drafting of the article; Takeshi Muneta: obtaining of funding, provision of study materials and patients; Kunikazu Tsuji: critical revision of the article for important intellectual content; Shizuko Ichinose: electron microscopy; Ichiro Sekiya: conception and design, critical revision of the article for important intellectual content, final approval of the article, obtaining of funding.

Conflict of interest

The authors have no conflict of interest.

Acknowledgement

This study was supported by grants from the Japanese Ministry of Education Global Center of Excellence (GCOE) Program, the International Research Center for Molecular Science in Tooth and Bone Diseases and from the Japan Society for the Promotion of Science (21591914) to TM and by the Japan Society for the Promotion of Science (21591914) to IS Recombinant human bone morphogenetic protein-7 was kindly provided by Stryker Biotech.

References

1. Pittenger M, Mackay A, Beck S, Jaiswal R, Douglas R, Mosca J, *et al.* Multilineage potential of adult human mesenchymal stem cells. Science 1999;284(5411):143–7.
2. Prockop D. Marrow stromal cells as stem cells for nonhematopoietic tissues. Science 1997;276(5309):71–4.
3. Sekiya I, Larson B, Smith J, Pochampally R, Cui J, Prockop D. Expansion of human adult stem cells from bone marrow stroma: conditions that maximize the yields of early progenitors and evaluate their quality. Stem Cells 2002;20(6):530–41.
4. Sakaguchi Y, Sekiya I, Yagishita K, Muneta T. Comparison of human stem cells derived from various mesenchymal tissues: superiority of synovium as a cell source. Arthritis Rheum 2005;52(8):2521–9.
5. Shirasawa S, Sekiya I, Sakaguchi Y, Yagishita K, Ichinose S, Muneta T. *In vitro* chondrogenesis of human synovium-derived mesenchymal stem cells: optimal condition and comparison with bone marrow-derived cells. J Cell Biochem 2006;97(1):84–97.
6. Yoshimura H, Muneta T, Nimura A, Yokoyama A, Koga H, Sekiya I. Comparison of rat mesenchymal stem cells derived from bone marrow, synovium, periosteum, adipose tissue, and muscle. Cell Tissue Res 2007;327(3):449–62.
7. Nimura A, Muneta T, Koga H, Mochizuki T, Suzuki K, Makino H, *et al.* Increased proliferation of human synovial mesenchymal stem cells with autologous human serum: comparisons with bone marrow mesenchymal stem cells and with fetal bovine serum. Arthritis Rheum 2008;58(2):501–10.
8. Mochizuki T, Muneta T, Sakaguchi Y, Nimura A, Yokoyama A, Koga H, *et al.* Higher chondrogenic potential of fibrous synovium- and adipose synovium-derived cells compared with subcutaneous fat-derived cells: distinguishing properties of mesenchymal stem cells in humans. Arthritis Rheum 2006;54(3):843–53.
9. Nagase T, Muneta T, Ju YJ, Hara K, Morito T, Koga H, *et al.* Analysis of the chondrogenic potential of human synovial stem cells according to harvest site and culture parameters in knees with medial compartment osteoarthritis. Arthritis Rheum 2008;58(5):1389–98.
10. Segawa Y, Muneta T, Makino H, Nimura A, Mochizuki T, Ju YJ, *et al.* Mesenchymal stem cells derived from synovium, meniscus, anterior cruciate ligament, and articular chondrocytes share similar gene expression profile. J Orthop Res 2009;27(4):435–41.
11. Brittberg M, Lindahl A, Nilsson A, Ohlsson C, Isaksson O, Peterson L. Treatment of deep cartilage defects in the knee with autologous chondrocyte transplantation. N Engl J Med 1994;331(14):889–95.
12. Wakitani S, Goto T, Pineda S, Young R, Mansour J, Caplan A, *et al.* Mesenchymal cell-based repair of large, full-thickness defects of articular cartilage. J Bone Joint Surg Am 1994;76(4):579–92.
13. Koga H, Shimaya M, Muneta T, Nimura A, Morito T, Hayashi M, *et al.* Local adherent technique for transplanting mesenchymal stem cells as a potential treatment of cartilage defect. Arthritis Res Ther 2008;10(4):R84.
14. Docheva D, Popov C, Mutschler W, Schieker M. Human mesenchymal stem cells in contact with their environment: surface characteristics and the integrin system. J Cell Mol Med 2007;11(1):21–38.
15. Hynes R. Integrins: bidirectional, allosteric signaling machines. Cell 2002;110(6):673–87.
16. Martino M, Mochizuki M, Rothenfluh D, Rempel S, Hubbell J, Barker T. Controlling integrin specificity and stem cell differentiation in 2D and 3D environments through regulation of fibronectin domain stability. Biomaterials 2009;30(6):1089–97.
17. Leitinger B, McDowall A, Stanley P, Hogg N. The regulation of integrin function by Ca2+. Biochim Biophys Acta 2000;1498(2–3):91–8.
18. Banères JL, Roquet F, Martin A, Parello J. A minimized human integrin alpha 5 beta 1 that retains ligand recognition. J Biol Chem 2000;275(8):5888–903.
19. Kirchhofer D, Grzesiak J, Pierschbacher MD. Calcium as a potential physiological regulator of integrin-mediated cell adhesion. J Biol Chem 1991;266(7):4471–7.
20. Grzesiak J, Davis G, Kirchhofer D, Pierschbacher M. Regulation of alpha 2 beta 1-mediated fibroblast migration on type I collagen by shifts in the concentrations of extracellular Mg2+ and Ca2+. J Cell Biol 1992;117(5):1109–17.
21. Ichinose S, Tagami M, Muneta T, Sekiya I. Morphological examination during *in vitro* cartilage formation by human mesenchymal stem cells. Cell Tissue Res 2005;322(2):217–26.

22. Moran DT, Rowley JC. Visual Histology. Philadelphia: Lea and Febiger; 1988.
23. Cross PC, Mercer KL. Cell and Tissue Ultrastructure: a Functional Perspective. New York: W.H. Freeman and Company; 1993.
24. Friedenstein AJ. Precursor cells of mechanocytes. Int Rev Cytol 1976;47:327–59.
25. Sekiya I, Colter DC, Prockop DJ. BMP-6 enhances chondrogenesis in a subpopulation of human marrow stromal cells. Biochem Biophys Res Commun 2001;284(2):411–8.
26. Sakaguchi Y, Sekiya I, Yagishita K, Ichinose S, Shinomiya K, Muneta T. Suspended cells from trabecular bone by collagenase digestion become virtually identical to mesenchymal stem cells obtained from marrow aspirates. Blood 2004;104(9):2728–35.
27. Song SW, Chang W, Song BW, Song H, Lim S, Kim HJ, *et al.* Integrin-linked kinase is required in hypoxic mesenchymal stem cells for strengthening cell adhesion to ischemic myocardium. Stem Cells 2009;27(6):1358–65.
28. Wayner E, Carter W. Identification of multiple cell adhesion receptors for collagen and fibronectin in human fibrosarcoma cells possessing unique alpha and common beta subunits. J Cell Biol 1987;105(4):1873–84.
29. Berdichevsky F, Alford D, D'Souza B, Taylor-Papadimitriou J. Branching morphogenesis of human mammary epithelial cells in collagen gels. J Cell Sci 1994;107(12):3557–68.
30. Carter W, Wayner E, Bouchard T, Kaur P. The role of integrins alpha 2 beta 1 and alpha 3 beta 1 in cell–cell and cell–substrate adhesion of human epidermal cells. J Cell Biol 1990;110 (4):1387–404.
31. Sekiya I, Vuoristo JT, Larson BL, Prockop DJ. *In vitro* cartilage formation by human adult stem cells from bone marrow stroma defines the sequence of cellular and molecular events during chondrogenesis. Proc Natl Acad Sci U S A 2002;99 (7):4397–402.
32. Sekiya I, Larson BL, Vuoristo JT, Reger RL, Prockop DJ. Comparison of effect of BMP-2, -4, and -6 on *in vitro* cartilage formation of human adult stem cells from bone marrow stroma. Cell Tissue Res 2005;320(2):269–76.
33. Koga H, Muneta T, Nagase T, Nimura A, Ju Y, Mochizuki T, *et al.* Comparison of mesenchymal tissues-derived stem cells for *in vivo* chondrogenesis: suitable conditions for cell therapy of cartilage defects in rabbit. Cell Tissue Res 2008;333 (2):207–15.

Threshold in Stage-specific Embryonic Glycotypes Uncovered by a Full Portrait of Dynamic *N*-Glycan Expression during Cell Differentiation*

Maho Amano‡, Misa Yamaguchi‡, Yasuhiro Takegawa‡, Tadashi Yamashita‡, Michiyo Terashima§, Jun-ichi Furukawa‡, Yoshiaki Miura¶, Yasuro Shinohara‡, Norimasa Iwasaki§, Akio Minami§, and Shin-Ichiro Nishimura‡¶‖

Although various glycoforms appear to participate independently in multiple molecular interactions in cellular adhesion that contribute to embryogenesis and organogenesis, a full portrait of the glycome diversity and the effect of the structural variations of cellular glycoforms on individual cell stages in proliferation and differentiation remain unclear. Here we describe a novel concept for the characterization of dynamic glycoform alteration during cell differentiation by means of "glycoblotting-based cellular glycomics," the only method allowing for rapid and quantitative glycan analysis. We demonstrated that processes of dynamic cellular differentiation of mouse embryonic carcinoma cells, P19CL6 and P19C6, and mouse embryonic stem cells into cardiomyocytes or neural cells can be monitored and characterized quantitatively by profiling entire *N*-glycan structures of total cell glycoproteins. Whole *N*-glycans enriched and identified by the glycoblotting method (67 glycans for P19CL6, 75 glycans for P19C6, and 72 glycans for embryonic stem cells) were profiled and bar-coded quantitatively with respect to the ratio of subgroups composed of characteristic glycoforms, namely glycotypes. ***Molecular & Cellular Proteomics 9:523–537, 2010.***

The global characterization of the genome, transcriptome, epigenome, and proteome of embryonic stem cells (ESCs)[1] has contributed to basic understanding of ESC biology (1). Functional genomics and proteomics during cellular differentiation have also been intensively studied during recent years (2–4). However, it was suggested that there is no significant change of the protein expression profile in the differentiated cells in comparison with that of undifferentiated (progenitor) cells. It is generally recognized that work on ESCs has proceeded with a general lack of standards for adequate quantification of ESCs (5). It is likely that this has led to inconsistencies and difficulties in reproducing work from independent laboratories because this field has relied upon a variety of antibodies against a few cell surface antigens, which has been useful but not adequate. Therefore, it should be noted that there has been no reliable set of molecular markers that can easily establish the quality and differentiation status of a cell line.

Numerous important roles of mammalian glycans are now evident, and the variation in the cellular glycome is a molecular basis for modulating dynamic cellular mechanisms such as cell-cell adhesion, cell activation, and malignant alterations (6–9). Structural variations of the glycome in cell surface glycoproteins and/or glycosphingolipids appear to produce some useful biomarkers such as stage-specific embryonic antigens and ligands for endogenous lectins during cell proliferation and differentiation (10–13). Loss of some key *N*-glycans or expression of unusual *N*-glycans disrupts normal cell-cell adhesion in early mammalian embryos that is associated with fertilization (14–17). In addition, it seems likely that cellular responsiveness to growth or arrest is greatly dependent on total *N*-glycan number and the degree of branching of cell surface glycoproteins (12). Judging from the fact that *N*-glycans found in most proteins are an overwhelming majority of the glycome compared with other subgroups such as *O*-glycans classified as mucin glycoproteins or glycosphingolipids, our attention should be focused on the expression profiles of cellular *N*-glycans.

We hypothesized that drastic changes in the ratio of some key subtypes of the *N*-glycans with mutual core structure against total *N*-glycan expression level may be crucial to

From the ‡Laboratory of Advanced Chemical Biology, Graduate School of Life Science, and Frontier Research Center for Post-Genome Science and Technology, Hokkaido University, N21 W11, Kita-ku, Sapporo 001-0021, Japan, §Department of Orthopedic Surgery, Hokkaido University School of Medicine, N15 W7, Kita-ku, Sapporo 060-8638, Japan, and ¶Ezose Sciences, Inc., Pine Brook, New Jersey 07058

Received, November 18, 2009, and in revised form, December 14, 2009

Published, MCP Papers in Press, December 14, 2009, DOI 10.1074/mcp.M900559-MCP200

[1] The abbreviations used are: ESC, embryonic stem cell; iPS, induced pluripotent stem; FBS, fetal bovine serum; RA, retinoic acid; HRP, horseradish peroxidase; NeuGc, *N*-glycolylneuraminic acid; HM, high mannose type; MF, monofucosylated type; DF, difucosylated type; O, others; BS, bisect type.

switch cell stages/types during cell differentiation in which generated *N*-glycan subtypes must exchange their major partner molecules in differentiated cell adhesion, namely cell surface carbohydrate-binding proteins or complementary glycans in sugar-sugar interaction (18). In other words, there might be a significant "threshold" or "critical point" in the expression level of the key *N*-glycan subtypes against cell surface area to initiate this dynamic cellular differentiation. For example, it is well documented that Lewis X trisaccharide antigen (SSEA-1), a prominent member of the Lewis blood group antigen family, is one of the most important subtypes that have key functional roles during developmental processes or cancer progression (10, 19). Glycosphingolipids SSEA-3 and SSEA-4 are also among the most commonly utilized markers to characterize ESCs, and they could also be classified as a sort of subtype composed of globoseries core oligosaccharide structures (13). Sialic acid-containing oligosaccharides are also supposed to be involved in some essential subtypes having various functions as potential markers in cell differentiation or malignant alteration (20). Therefore, it is not surprising that real time monitoring of entire *N*-glycan expression levels in the course of proliferation and differentiation, a full portrait of the cellular glycoforms, may allow for the identification of target cells and assessment of the quality of individual stem cells and differentiated cells. The advent of such a versatile and comprehensive protocol for quantitative cellular glycomics is now urgently needed because it should greatly contribute to the quality control of human ESCs and a variety of human induced pluripotent stem (iPS) cells in terms of the warranty of safety and reproducibility of required stem cell engineering (21–23).

Until now, technical limitations have restricted acquisition of the total glycan structures of mammalian cells and evaluation of the cell type-specific glycoforms (24). We report herein that the glycoblotting method (24), a PCR-like technology developed for rapid and large scale enrichment analysis of human serum glycans (25, 26), can be used for rapid and quantitative cellular glycomics to monitor dynamic glycoform alteration during differentiation of mouse embryonic carcinoma cells (P19CL6 and P19C6 cells) and mouse ESCs.

MATERIALS AND METHODS

Cell Culture and Differentiation—P19C6 and P19CL6 cells were subcloned from pluripotent mouse embryonal carcinoma, and both were obtained from RIKEN Cell Bank (Ibaragi, Japan) (27, 28). P19C6 and P19CL6 were maintained with Dulbecco's modified Eagle's medium (Sigma-Aldrich) supplemented with 15% fetal bovine serum (FBS; Biological Industries, Kibbutz Beit Haemek, Israel) and minimum Eagle's medium α supplemented with 10% FBS and penicillin-streptomycin (Invitrogen), respectively, at 37 °C in an atmosphere of 5% CO_2. P19C6 cells were differentiated as described by Tang and co-workers (29). In brief, P19 cells were cultured by the hanging drop method and allowed to aggregate in bacterial grade Petri dishes at a cell density of 1×10^5 cells/ml in the presence of 1 μM retinoic acid (RA) (Sigma) in minimum Eagle's medium α supplemented with 10% FBS. After 4 days of aggregation, cells were collected in "aggregate," an intermediate of differentiation, by treatment with 0.05% trypsin, EDTA (Invitrogen) and were replated onto a poly-L-lysine-coated tissue culture dish (6 cm inner diameter) at a density of 5×10^4 cells/cm^2 in Dulbecco's modified Eagle's medium/F-12 medium (Invitrogen) containing N-2 supplement and fibronectin. The cells were then allowed to adhere and were cultured for 5 days. Cardiac muscle differentiation of P19CL6 cells was induced by DMSO under adherent conditions as described previously (27). Briefly, 3.7×10^5 cells were plated onto a tissue culture dish (6 cm inner diameter) (Corning) and cultured in a standard medium containing 1% DMSO for 16 days. As a control, undifferentiated cells were cultured in standard medium for 16 days. The media were changed every 2 days. All experiments were performed in triplicate and repeated twice independently ($n = 6$). Mouse ESCs were differentiated under conditions reported previously (30, 31).

Basic Protocol of Glycoblotting-based Quantitative Cellular N-Glycomics—A preliminary trial for the cellular *N*-glycomics was reported previously in human prostate cancer cells (PC-3) and normal human prostate epithelial cells on the basis of the protocol designed for human serum *N*-glycomics using the BlotGlyco™ ABC bead, a prototype bead prepared by conjugating *N*-(2-aminobenzoyl)cysteine hydrazide and thiopropyl-Sepharose 6B (26). However, we had to re-examine and establish a comprehensive protocol feasible for mammalian cellular glycomics using BlotGlyco H, a commercially available synthetic polymer bead (Sumitomo Bakelite Co., Ltd., Tokyo, Japan) (see Fig. 1), because our recent studies on the functional glycomics using BlotGlyco H bead have demonstrated improved performance of this new platform in terms of quantification, reproducibility, and application (25).

Release of total *N*-glycans was carried out directly using whole cell lysates as follows. After inducing differentiation, P19C6 and ESCs were cultured by using a poly-L-lysine-coated tissue culture dish (6 cm inner diameter) for the appropriate days indicated above, then were scraped in PBS containing 10 mM EDTA, and washed with PBS. Following suspension in PBS, cells were lysed by incubation with 1% Triton X-100 for 1 h on ice. The lysates were centrifuged at 15,000 rpm for 10 min at 4 °C, and the obtained supernatant was added to cold acetone (1:4) to precipitate proteinaceous materials. The precipitates were collected by centrifugation at 12,000 rpm for 15 min at 4 °C followed by serial washing with acetonitrile. The resulting precipitates were dissolved in 50 μl of 80 mM ammonium bicarbonate containing 0.2% of 1-propanesulfonic acid, 2-hydroxyl-3-myristamido and incubated at 60 °C for 10 min. The solubilized proteinaceous materials were reduced by 10 mM DTT at 60 °C for 30 min followed by alkylation with 20 mM iodoacetamide by incubation in the dark at room temperature for 30 min. The mixture was then treated with 400 units of trypsin (Sigma-Aldrich) at 37 °C overnight followed by heat inactivation of the enzyme at 90 °C for 10 min. After cooling to room temperature, *N*-glycans of glycopeptides were released from trypsin-digested samples by incubation with 2 units of peptide-*N*-glycosidase F (Roche Applied Science) at 37 °C overnight. Then the sample mixture was dried by SpeedVac and stored at −20 °C until use. Approximately 1–5 $\times 10^6$ cells (~200 μg of total protein) corresponding to cell confluence on the culture dish (6 cm inner diameter) were required for this procedure.

Glycoblotting of the sample mixtures containing whole cell *N*-glycans by means of BlotGlyco H bead was performed according to the procedure described previously (26). BlotGlyco H beads (500 μl) (10 mg/ml suspension; Sumitomo Bakelite Co., Ltd.) were aliquoted onto a well of a MultiScreen Solvinert filter plate (Millipore, Billerica, MA). Peptide-*N*-glycosidase F-digested samples were dissolved with 20 μl of water and applied to the well followed by the addition of 180 μl of 2% acetic acid in ACN. The plate was incubated at 80 °C for 45 min to capture total glycans in sample mixtures specifically onto